

## Role of thermodynamic relaxation on effectiveness of recycling agents on properties of aged bitumen

Ren, Shisong; Liu, Xueyan; Erkens, Sandra

**DOI**

[10.1016/j.fuel.2024.131658](https://doi.org/10.1016/j.fuel.2024.131658)

**Publication date**

2024

**Document Version**

Final published version

**Published in**

Fuel

**Citation (APA)**

Ren, S., Liu, X., & Erkens, S. (2024). Role of thermodynamic relaxation on effectiveness of recycling agents on properties of aged bitumen. *Fuel*, 368, Article 131658. <https://doi.org/10.1016/j.fuel.2024.131658>

**Important note**

To cite this publication, please use the final published version (if applicable). Please check the document version above.

**Copyright**

Other than for strictly personal use, it is not permitted to download, forward or distribute the text or part of it, without the consent of the author(s) and/or copyright holder(s), unless the work is under an open content license such as Creative Commons.

**Takedown policy**

Please contact us and provide details if you believe this document breaches copyrights. We will remove access to the work immediately and investigate your claim.



## Full Length Article

# Role of thermodynamic relaxation on effectiveness of recycling agents on properties of aged bitumen

Shisong Ren<sup>\*</sup>, Xueyan Liu, Sandra Erkens

Section of Pavement Engineering, Delft University of Technology, Stevinweg 1, 2628 CN Delft, the Netherlands

## ARTICLE INFO

## Keywords:

Rejuvenated bitumen  
Molecular dynamic simulation  
Low-temperature performance  
Thermodynamic indicator  
Multi-scale connection

## ABSTRACT

The low-temperature relaxation and fatigue cracking performance are two essential aspects in estimating the rejuvenation efficiency of recycling agents (RAs). This study aims to fundamentally investigate the effects of recycling agent type/dosage and aging degree of bitumen on thermodynamic and rheological properties of rejuvenated bitumen at low and intermediate temperatures. Molecular dynamics (MD) simulations are utilized to predict thermodynamic indices of rejuvenated bitumen, further linked to critical low-temperature and fatigue indicators from experiments. The results reveal that all RAs show a regeneration effect on fractional free volume (FFV), self-diffusion coefficient ( $D_s$ ), glass transition temperature ( $T_g$ ), and surface free energy ( $\gamma$ ). Bio-oil and engine-oil exhibit higher rejuvenation efficiency on these thermodynamic properties than naphthenic-oil and aromatic-oil. The aging degree of bitumen and temperature show significant effects on rejuvenation efficiency. It is recommended to use the FFV parameter to predict the relaxation properties of rejuvenated bitumen. However, these thermodynamic indicators inadequately differentiate between rejuvenators and softeners. Based on crossover parameter results, most recycling agents (bio-oil, engine oil, and naphthenic oil) in this study display softening characteristics. Only aromatic oil effectively rejuvenates the crossover modulus ( $G_c$ ) of aged binder. Notably, engine oil demonstrates the least rejuvenation in crossover parameters for the recovery of aged bitumen. Further,  $\gamma$  demonstrates a strong association with both Glover-Rowe (G-R) and fatigue crack width  $C_{500}$  indices across all cases involving rejuvenated bitumen. This work will build a multi-scale evaluation framework on the rejuvenation effectiveness of recycling agents on low-temperature and fatigue performance of aged bitumen.

## 1. Introduction

In the Netherlands, the Sustainable Road Pavement Transition Path proposes to work on climate-neutral and 100 % circular, with high-quality reuse of all materials and halving the use of primary raw materials, but with the high-quality standard that we are used to [1]. The concept of sustainable circulation expects that about 70 % of reclaimed porous asphalt waste materials will be reused by 2030 [2]. To ensure the satisfactory engineering performance of reclaimed asphalt pavement, recycling agents must be added [3,4]. Therefore, the development of high-efficiency rejuvenation technologies is crucial; however, challenges persist, particularly in the realms of inconsistent rejuvenation efficiency assessment methods and the obscure understanding of rejuvenation mechanisms across recycling agent and aged bitumen [5].

However, it is insufficient to build a comprehensive design-production-evaluation framework on rejuvenated bitumen only with

macroscopic tests [6]. The resource and component diversity of both recycling agent and aged bitumen will lead to extensive rheological and mechanical tests [7]. In other words, it is necessary to fundamentally understand the rejuvenation mechanisms of variable rejuvenated bitumen blends and exploit a multiscale evaluation framework. To this end, researchers have carried out molecular-scale characterizations and simulations on various rejuvenated binders [8,9]. The molecular dynamics (MD) simulations are popularly utilized to fundamentally explore the rejuvenation efficiency and mechanism of rejuvenated bitumen. Table 1 provides an overview of current research on MD simulations applied to rejuvenated bitumen systems. This summary includes details on the chosen recycling agents and aged bitumen model, performance evaluation criteria, output indicators generated through MD simulations, and the potential analysis of the relationship between MD simulation results and macroscale rheological and mechanical properties.

<sup>\*</sup> Corresponding author.

E-mail address: [Shisong.Ren@tudelft.nl](mailto:Shisong.Ren@tudelft.nl) (S. Ren).

<https://doi.org/10.1016/j.fuel.2024.131658>

Received 16 September 2023; Received in revised form 22 January 2024; Accepted 4 April 2024

Available online 7 April 2024

0016-2361/© 2024 The Author(s). Published by Elsevier Ltd. This is an open access article under the CC BY license (<http://creativecommons.org/licenses/by/4.0/>).

**Table 1**  
MD simulation cases on rejuvenated bitumen systems.

Recycling agents	Aged bitumen	Influence factor	Evaluation indicators	Ref
Waste cooking oil	Aged SBS-bitumen	Temperature	MSD, D, $T_g$ , CED, $\gamma$ , RDF, FFV, G, K, E, and $\nu$	[10]
Waste cooking oil	AAA-1 model	WCO components	ESP, Dipole moment, $\rho$ , CED, SP, $\gamma$ , Energy constructions, FFV, D	[11]
Diocetyl phthalate, Tributyl citrate acetate, Oleic; Oleamide; Undecane and saturated naphthene	12-component model	Chemical components	MSD; RDF; $E_{interaction}$ , D, $\eta$ , Tensile stress	[12]
Single component $C_{12}H_{16}$	12-component model	Recycling agent (RA) dosage, moisture, temperature	$\rho$ , $\eta$ , K, $\gamma$ , Waa, RDF, $W_{adhesion}$ , $W_{debonding}$ , MSD, D	[13]
Poly-sulfide	Aged SBS-bitumen	RA dosage	D, $\eta$ , SP	[14]
Paraffin	12-component model	RA dosage	G, K, E, and $\nu$ , MSD, D	[15]
Vegetable oil	3-component model	Chemical component, temperature	$\rho$ , D, RDF, thermal conductivity, $\eta_0$	[16]
Straight-chains and aromatics	12-component model	–	$\rho$ , $T_g$ , RDF, CED, SP, concentration profile,	[17]
Hexadecanamide (palmitic amide)	Asphaltene agglomeration	Temperature	Optimum distance (d), and vertical distance ( $d_{ver}$ )	[18]
Soybean-oil	Four-component model	RA dosage, Temperature	D, SP, Adsorption energy ( $E_a$ ), RDF	[19]
–	12-component model	Bitumen components	$\rho$ , $T_g$ , FFV, MSD, D, RDF	[20]
Naphthene aromatic, cyclic saturates, straight saturates	AAA-1 model	RA type	D, CED, SP, Energetic indices	[21]
Typical regenerator ( $C_{12}H_{16}$ )	Aged crumb rubber bitumen	–	CED, SP, RDF,	[22]

Note: MSD-mean square displacement,  $D(\rho)$ -density,  $T_g$ -glass transition temperature, CED-cohesive energy density,  $\gamma$ -surface free energy, RDF-radial distribution function, FFV-fractional free volume, G-bulk modulus, K-shear modulus, E-elastic modulus, SP-solubility parameter,  $E_{interaction}$ -interaction energy,  $\eta$ -viscosity, Waa-work of cohesion,  $\eta_0$ -zero-shear viscosity.

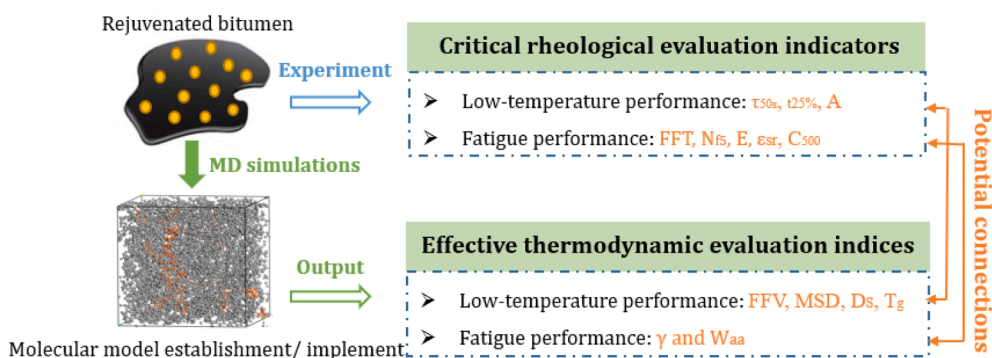


**Fig. 1.** Graph illustration of research structure.

Although the recycling agent (RA) type, influence factors, and evaluation indicators involved in MD simulation studies are different, the general conclusion was drawn that the addition of RA molecules would enhance these thermodynamic indicators and molecular distribution (especially for asphaltene clusters [12,21]) of aged bitumen more or less. However, existing MD simulation studies have solely focused on determining whether the inclusion of RA molecules could reinstate the thermodynamic and structural characteristics of aged bitumen model while elucidating the molecular-level rejuvenation mechanism. Limited work has been conducted to systematically investigate the influence of RA type/dosage and aging level of bitumen on MD simulation results, and the effective thermodynamic indices for rejuvenation efficiency evaluation of different rejuvenated bitumen models are still inconsistent and unclear. Meanwhile, MD simulation studies are always implemented solely with fewer connections with experimental rheological and mechanical properties of rejuvenated bitumen. As a result, MD simulations on rejuvenated bitumen are currently in the research phase and offer limited advantages in terms of guiding the evaluation, optimization, and utilization of RAs.

The primary aim of this study is to gain a comprehensive understanding of how various recycling agents affect the molecular-scale rejuvenation efficiency and mechanism, specifically concerning the low-temperature performance and fatigue behavior of aged bitumen. It is expected to propose effective thermodynamic indices outputted from molecular dynamics simulations for rejuvenation efficiency evaluation, closely related to macroscale critical rheological indicators measured

from tests. The main research structure is illustrated in Fig. 1. The study aims to develop molecular models for rejuvenated bitumen, considering various recycling agent types, dosages, and bitumen aging levels, to predict their thermodynamic parameters. The research will assess the effectiveness of these thermodynamic parameters in efficiently evaluating and distinguishing the rejuvenation effects of different recycling agents. Simultaneously, rheological tests will be conducted to evaluate the crucial low-temperature and fatigue characteristics of rejuvenated bitumen. Furthermore, the potential correlations between the identified efficient thermodynamic evaluation indices and essential rheological evaluation metrics for rejuvenated binders will be explored.

## 2. Materials and experimental tests

### 2.1. Materials and sample preparation

In this study, 70/100 fresh bitumen was utilized to prepare aged and rejuvenated binders, and its basic properties are listed in Table 2. Meanwhile, four types of recycling agents (RAs) within different categories were used and named bio-oil (BO), engine-oil (EO), naphthenic-oil (NO), and aromatic-oil (AO). Their physical and chemical properties are shown in Table 3.

The fresh bitumen was treated with short- and long-term aging procedures by the Thin Film Oven test (TFOT) and Pressure Aging Vessel (PAV). The temperature and aging time in the TFOT test were 163°C and 5 h, while temperature and pressure in the PAV test were 100°C and 2.1

**Table 2**  
The properties of fresh 70/100 bitumen.

Items	Properties	Value	Test standard
Physical indicators	Density (25°C, g/cm <sup>3</sup> )	1.017	EN 15,326
	Penetration (25°C, 1/10 mm)	91	ASTM D35
	Softening point (°C)	48.0	ASTM D36
	Viscosity (135°C, Pa·s)	0.80	AASHTO T316
	Carbon C (wt%)	84.06	
Element analysis	Hydrogen H (wt%)	10.91	
	Nitrogen N (wt%)	0.90	ASTM D7343
	Oxygen O (wt%)	0.62	
	Sulfur S (wt%)	3.52	
	Asphaltene As (wt%)	12.8	
SARA fractions	Resin R (wt%)	30.3	ASTM D4124
	Aromatic A (%)	53.3	
	Saturate S (%)	3.6	
Mechanical properties (60°C, 1.6 Hz)	Complex modulus G* (kPa)	2.4	AASHTO M320
	Phase angle $\delta$ (°)	84.5	

**Table 3**  
The physical and chemical indicators of four recycling agents.

Recycling agents	BO	EO	NO	AO	
Physical	Density (25°C, g/cm <sup>3</sup> )	0.911	0.833	0.875	0.994
	Viscosity (25°C, cP)	50	60	130	63,100
	Flash point (°C)	265–305	>225	>230	>210
	Nitrogen N (%)	0.15	0.23	0.12	0.55
Chemical	Carbon C (%)	76.47	85.16	86.24	88.01
	Hydrogen H (%)	11.96	14.36	13.62	10.56
	Sulfur S (%)	0.06	0.13	0.10	0.48
	Oxygen O (%)	11.36	0.12	0.10	0.40
	Mn (g/mol)	286.43	316.48	357.06	409.99

MPa, respectively. The long-term aging time varied from 20 h to 40 h and 80 h, and the aged bitumen was abbreviated with LAB20, LAB40, and LAB80 [25].

Three aged bitumen were firstly preheated to 160°C, and four RAs (BO, EO, NO, and AO) were blended for 10 min to manufacture the rejuvenated bitumen (BORB, EORB, NORB, and AORB). In LAB40

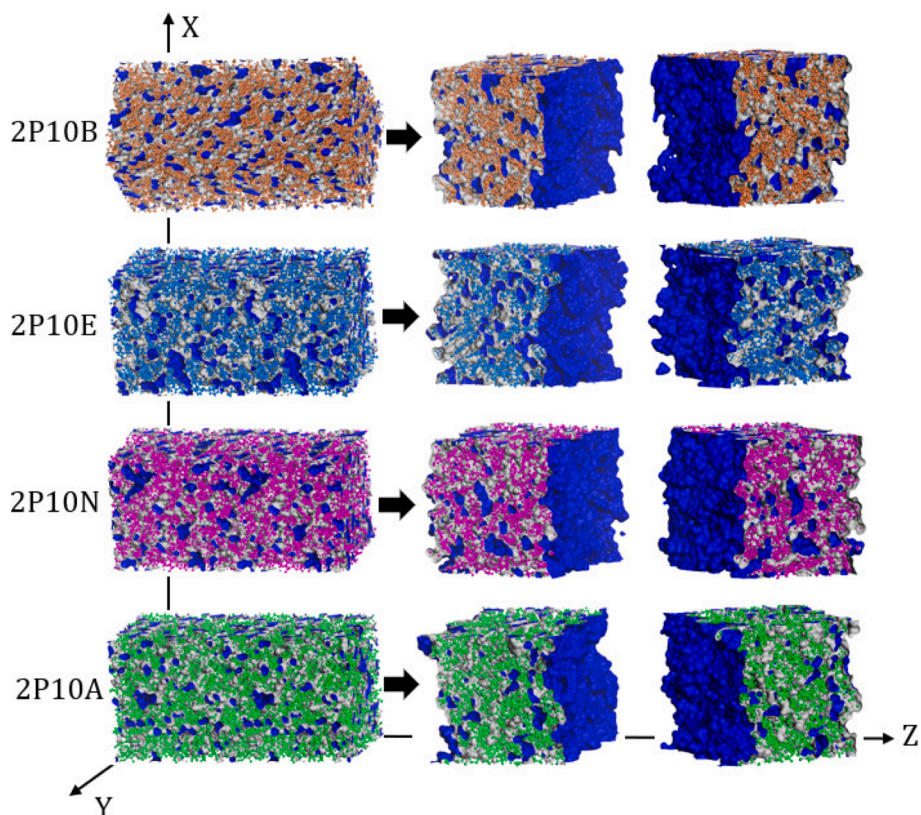


**Fig. 2.** Bulk (left) and Confined (right) molecular models of 2P10 rejuvenated bitumen.



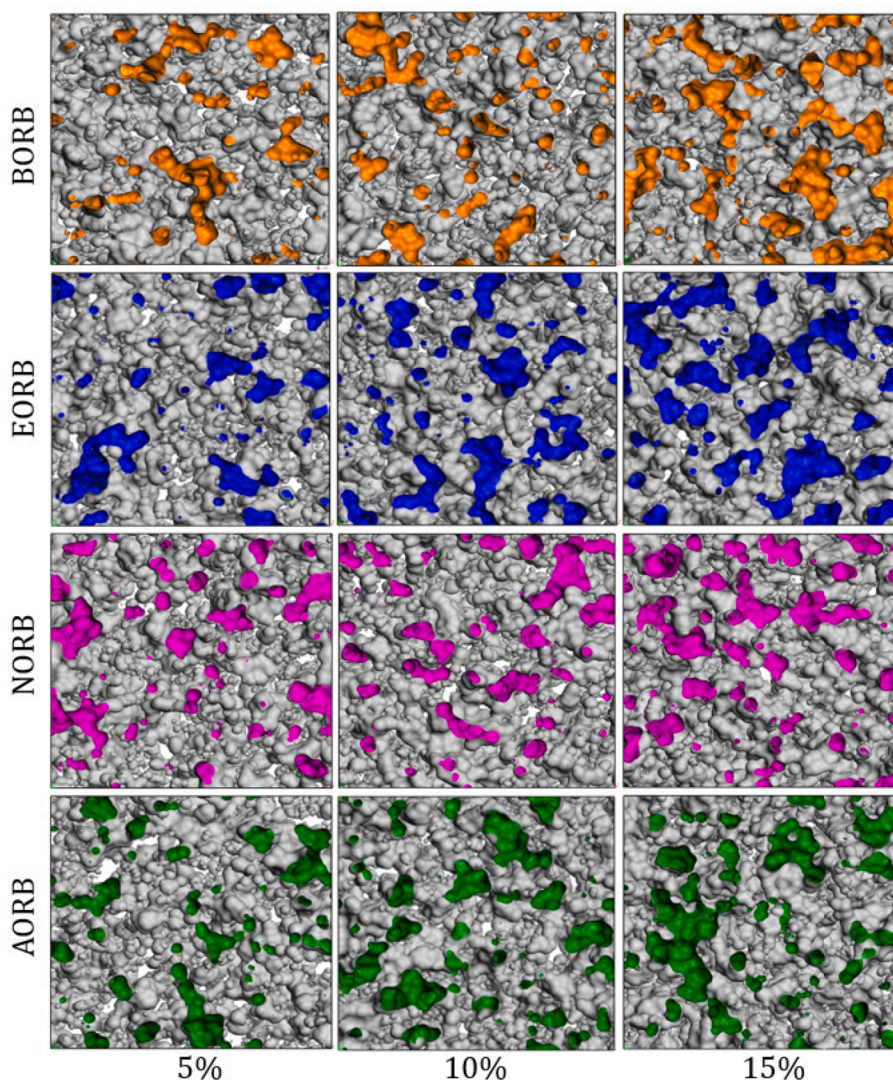


Fig. 3. Volumetric illustration of rejuvenated bitumen versus RA dosage at 333 K.

rejuvenated bitumen, the RA dosage increases from 5 % to 15 % with an interval of 2.5 %. Meanwhile, the content was 10 % in both LAB40 and LAB80 binders to see the effect of bitumen aging level. It should be noted that the abbreviation of one specific rejuvenated bitumen is composed of the aging level of bitumen and RA type/dosage. The 2P10B rejuvenated bitumen was prepared by adding a 10 % bio-oil to LAB40-aged bitumen.

## 2.2. Experimental tests

The low-temperature relaxation test was conducted to measure the critical relaxation parameters ( $\tau_{50\%}$ ,  $t_{25\%}$ , A) of different rejuvenated bitumen. Meanwhile, the frequency sweep test was performed to build master curves and determine the crossover parameters (crossover frequency  $f_c$  and crossover modulus  $G_c$ ) and Glover-Rowe (G-R) values of all bitumen binders. Regarding the fatigue behaviors, the linear viscoelastic test, linear amplitude sweep (LAS) test, and time sweep test (TS) were performed to determine the FFT,  $N_{f5}$ ,  $E$ ,  $\epsilon_{sr}$ , and  $C_{500}$  values. Detailed information on test conditions and definition of these critical indicators can be found in our published papers [22–24].

## 3. Molecular models' establishment of rejuvenated bitumen

To mitigate any potential impact stemming from the MD simulation protocol, the procedure for generating rejuvenated bitumen aligns with

that utilized for aged binders as outlined in our previous work [25,26]. In this study, 28 rejuvenated bitumen samples with variable recycling agent type, dosage, and aging degree of bitumen were subjected to the MD simulations, and their MD simulation protocols were the same as discussed above. The model information of virgin, aged, and rejuvenated binders is listed in Table S1. Concurrently, the number of different atoms (carbon C, hydrogen H, nitrogen N, oxygen O, and sulfur S), overall molecular count, molecular weight, and volume of all rejuvenated bitumen models are also summarized. The bulk models of 2P10B, 2P10E, 2P10N, and 2P10A are displayed in Fig. 2.

Apart from bulk molecular models, a distinct set of confined models has been built to assess their surface energy and work of cohesion. The chemical constituents and MD simulation protocols employed in the confined models are the same as the corresponding bulk models of rejuvenated bitumen. The sole discrepancy between these confined and bulk models is the boundary condition applied along the Z-axis, as depicted in Fig. 2. Due to the absence of a boundary along the Z axis in the confined model (substituted by vacuum layer), two additional confined surfaces are created in a confined model in this direction (displayed in blue). The surface energy can be computed based on the difference in model energies and surface area between bulk and confined models.

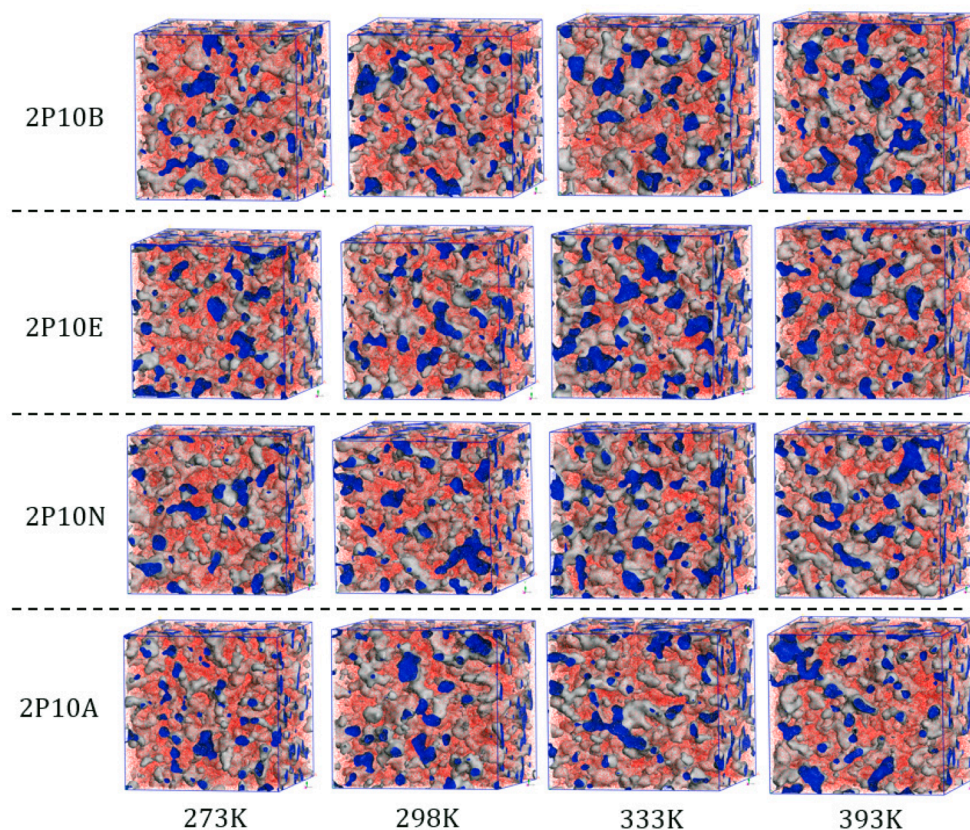


Fig. 4. Volumetric illustration of rejuvenated bitumen versus temperature.

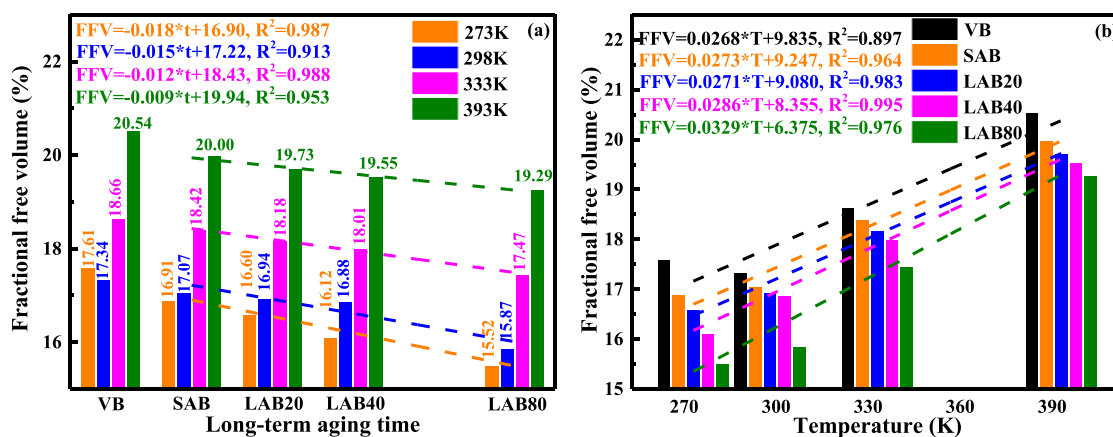


Fig. 5. Fractional free volume of virgin and aged bitumen at different temperatures.

#### 4. Molecular-scale evaluation indicators from MD simulations

##### 4.1. Volumetric parameters

The volumetric parameters outputted from MD simulations contain the total volume  $V_T$ , occupied volume  $V_O$ , and free volume  $V_F$ . The total volume refers to the whole equilibrate simulation model volume, while the occupied and free volumes come from the molecular intrinsic volume and intermolecular space, respectively. The free volume is the most important index to determine the volume variation of the recycling agent system. However, it is difficult to directly compare the free volume of recycling agents (RAs) because their molecular structures result in the variable occupied and total volume. Herein, an effective index, fractional free volume (FFV, %), is introduced to quantitatively compare the

free volume terms of various RAs, which is calculated as follows:

$$\text{FFV} = \frac{V_F}{V_T} = \frac{V_T - V_O}{V_T} \quad (1)$$

where  $V_T$ ,  $V_F$ , and  $V_O$  are the total volume, free volume, and occupied volume. The unit of these volumetric parameters is  $\text{\AA}^3$ .

##### 4.2. Dynamic properties

The dynamic capacity of rejuvenated bitumen molecules is reflected by the mean square displacement (MSD). It describes the path of molecular motion during the equilibrium NVT MD simulations, attributed to the Brownian self-movement and intermolecular interactions.



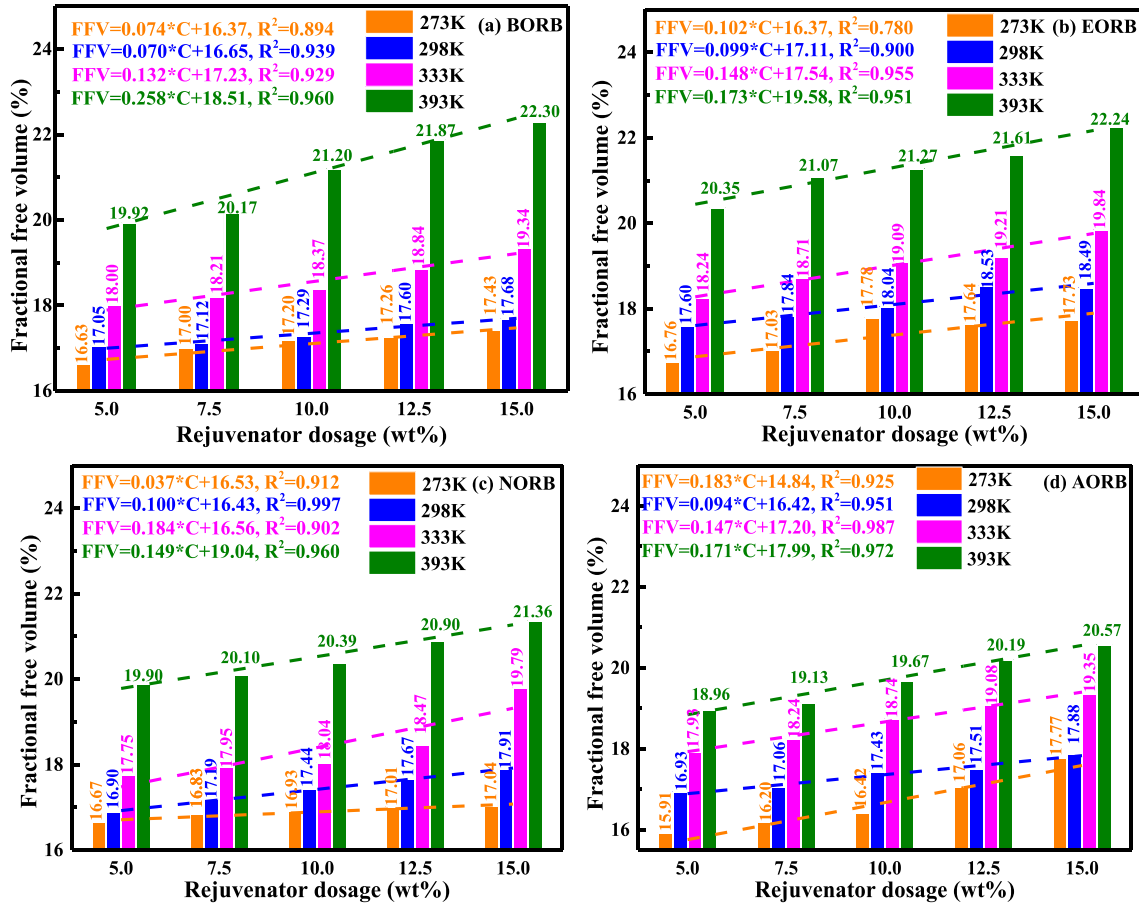


Fig. 6. FFV values versus RA dosage of different rejuvenate bitumen.

$$\text{MSD}(t) = \langle \Delta r_i(t)^2 \rangle = \langle [r_i(t) - r_i(0)]^2 \rangle \quad (2)$$

where  $\text{MSD}(t)$  is the mean square displacement of rejuvenated bitumen molecules at simulation time  $t$  (ps),  $\text{\AA}^2$ ;  $r_i(0)$  and  $r_i(t)$  refers to the initial and current coordinate,  $\text{\AA}$ .

The study tracks correlation curves between Mean Square Displacement (MSD) and simulation time ( $t$ ) for rejuvenated bitumen models. The MSD parameters of the bitumen models exhibit linearly increasing trends as simulation time progresses. To quantitatively assess the impact of adding RA molecules on the diffusive behavior of aged bitumen molecules, a self-diffusion coefficient indicator (DS) is introduced using Eq.3.

$$D_s = \frac{1}{6N} \lim_{t \rightarrow \infty} \frac{d}{dt} \sum \text{MSD}(t) = \frac{a}{6} \quad (3)$$

where  $D_s$  is the self-diffusion coefficient,  $\text{m}^2/\text{s}$ ;  $N$  refers to the total number of rejuvenated bitumen models; MSD represents the mean square displacement,  $\text{\AA}^2$ ;  $t$  is the simulation time, s; and  $a$  means the slope value in MSD-Time curves.

### 4.3. Glass transition temperature $T_g$

It was reported that there was a turning trend in temperature sensitivity of thermodynamic properties of bituminous materials before and after the  $T_g$  point. Meanwhile, the  $T_g$  value was strongly related to intermolecular interactions and free volume ratio. Thus, the variation trends of non-bond energy  $E_N$  and fractional free volume FFV as a function of temperature (varying from 210 K to 480 K) of different rejuvenated bitumen models after NPT and NVT equilibrium MD simulations are observed to detect their  $T_g$  values.

### 4.4. Surface free energy and work of cohesion

It is well-recognized that the surface characteristics (such as surface free energy) show great connections with both the cohesion and adhesion performance of bituminous materials. By establishing the confined models, the surface free energy  $\gamma$  and work of cohesion  $W_{aa}$  can be anticipated by using Eqs.4 and 5.

$$\gamma = (E_{\text{confined}} - E_{\text{bulk}})/2A \quad (4)$$

$$W_{aa} = 2\gamma \quad (5)$$

where  $E_{\text{confined}}$  and  $E_{\text{bulk}}$  refer to the potential energy of the confined model and bulk model of rejuvenated bitumen;  $A$  shows the generated new surface area,  $\text{mm}^2$ .

### 4.5. Rejuvenation percentage TRP calculation

To quantitatively assess the effects of different rejuvenation conditions (recycling agent type, dosage, and bitumen aging level) on the molecular-scale properties of aged bitumen, the rejuvenation percentage TRP of rejuvenated bitumen models is calculated as Eq.6.

$$\text{TRP} = \frac{T_{\text{aged}} - T_{\text{rejuvenated}}}{T_{\text{aged}} - T_{\text{fresh}}} * 100 \quad (6)$$

where TRP is the rejuvenation percentages based on MD simulation outputs, and  $T_{\text{aged}}$ ,  $T_{\text{rejuvenated}}$ , and  $T_{\text{fresh}}$  are thermodynamic properties of aged, rejuvenated, and fresh bitumen, respectively.

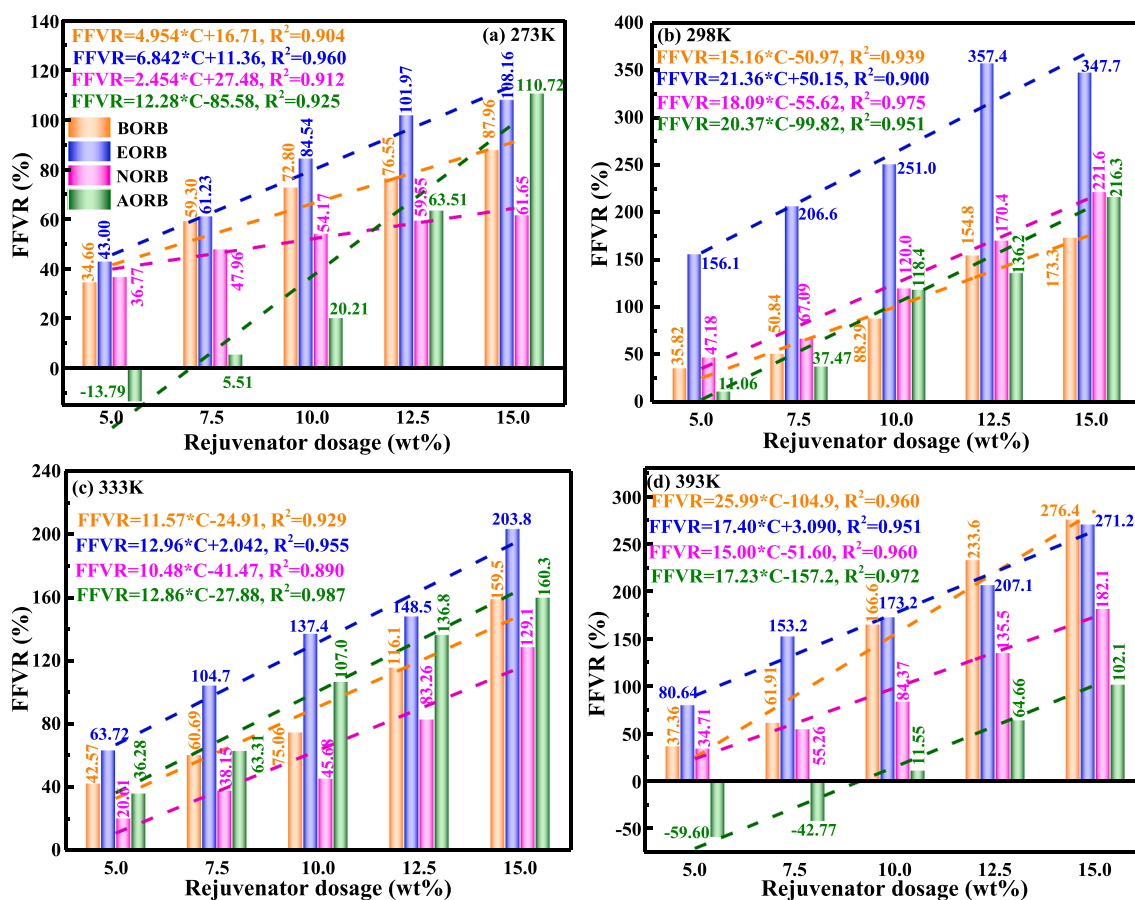


Fig. 7. FFVR values versus RA dosage of different rejuvenated bitumen.

## 5. MD simulation results and discussion

### 5.1. Volumetric parameters

Fig. 3 illustrates the volumetric characteristics of rejuvenated bitumen as a function of recycling agent (RA) dosage at 333 K. The grey particles represent the volume occupied by bitumen molecules, while the colored regions correspond to isosurfaces. Different colors are associated with distinct types of rejuvenated bitumen (Orange: Bio-oil; Blue: Engine-oil; Pink: Naphthenic-oil; Green: Aromatic-oil). The open spaces between the grey particles constitute the free volume, and it is evident that the free volume of rejuvenated bitumen expands as the RA dosage increases.

Additionally, for a closer examination of the temperature's impact on the volumetric properties of rejuvenated bitumen, the rejuvenated bitumen with LAB40 aging degree and a 10 % RA dosage is chosen for analysis. The results are displayed in Fig. 4. As the temperature rises, the free volume of rejuvenated bitumen increases gradually.

To quantitatively assess the rejuvenation effectiveness of recycling agents on volumetric parameters, the fractional free volume (FFV) of virgin, aged, and rejuvenated binders are estimated, and the results of virgin and aged bitumen are shown in Fig. 5. It is found that the FFV value of bitumen reduces linearly as the long-term aging time prolongs, but increases linearly as temperature rises. The aging process typically reduces the low-temperature relaxation capability of bitumen, whereas elevated temperatures positively influence its relaxation properties. With increasing temperature, the absolute slope values of FFV-t correlation equations decrease, indicating that the aging degree has a diminishing effect on FFV at higher temperatures. From the FFV-T curves, the temperature sensitivity of FFV values increases gradually as the aging degree of bitumen deepens.

The FFV values of various rejuvenated binders are plotted in Fig. 6. Due to the rejuvenation function, the addition of all recycling agents (RAs) enlarges the FFV values of aged bitumen, increasing linearly as the recycling agent (RA) content increases. That's why high RA dosage is beneficial in enhancing the relaxation properties of rejuvenated bitumen. It is observed that the RA type shows a great effect on the FFV values of rejuvenated bitumen. The BO and EO rejuvenated bitumen exhibit larger FFV values than the NO and AO rejuvenated bitumen, indicating that the BORB and EORB would show greater low-temperature performance than the NORB and AORB binders. This observation aligns closely with the results obtained from relaxation tests [24].

The FFV-based rejuvenation percentages of rejuvenated bitumen are calculated to investigate the FFV parameter feasibility as an effective index for assessing the rejuvenation efficiency of RAs. The results are displayed in Fig. 7. The FFVR values demonstrate a direct and proportional connection with the amount of RA dosage, suggesting that a higher RA dosage corresponds to a greater rejuvenation effect on FFV recovery in aged bitumen. Additionally, elevating the temperature appears to further enhance the FFVR values for rejuvenated bitumen. The FFVR ranges are  $-15$ – $120$  %,  $0$ – $360$  %,  $0$ – $210$  %, and  $0$ – $280$  % at 273 K, 298 K, 333 K, and 393 K, respectively. The magnitude of FFVR values is reasonable but higher than the rejuvenation percentage range based on relaxation parameters. Thus, it is easier for recycling agents to restore free volume ratio of aged bitumen at the molecular level than the macroscale low-temperature relaxation performance. The explanation could be that the low-temperature behavior of bitumen is connected not only to free volume but also to molecular motion and intermolecular interaction [31]. The EORB binders show the highest FFVR values, showing that engine-oil addition can mostly improve the free volume ratio in aged bitumen. However, there is no general conclusion obtained

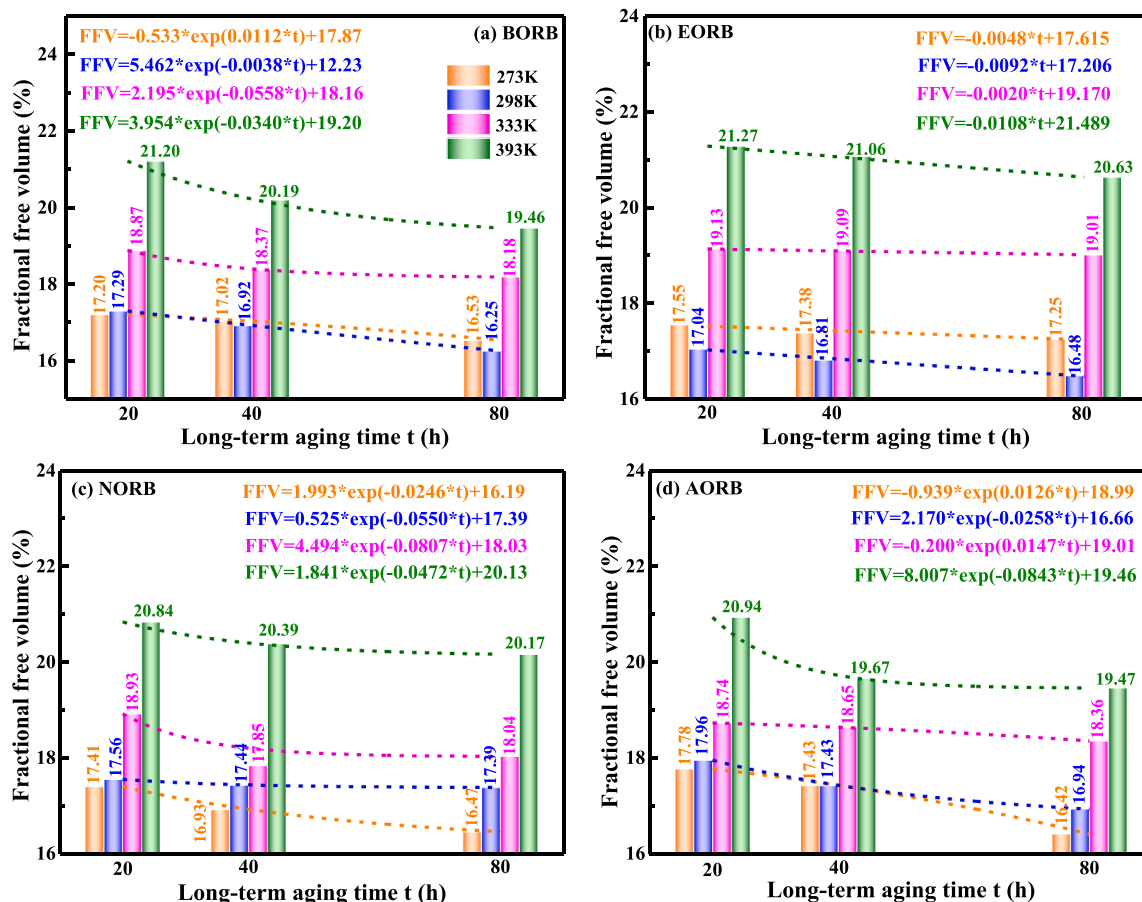


Fig. 8. Influence of aging time on FFV value of rejuvenated bitumen.

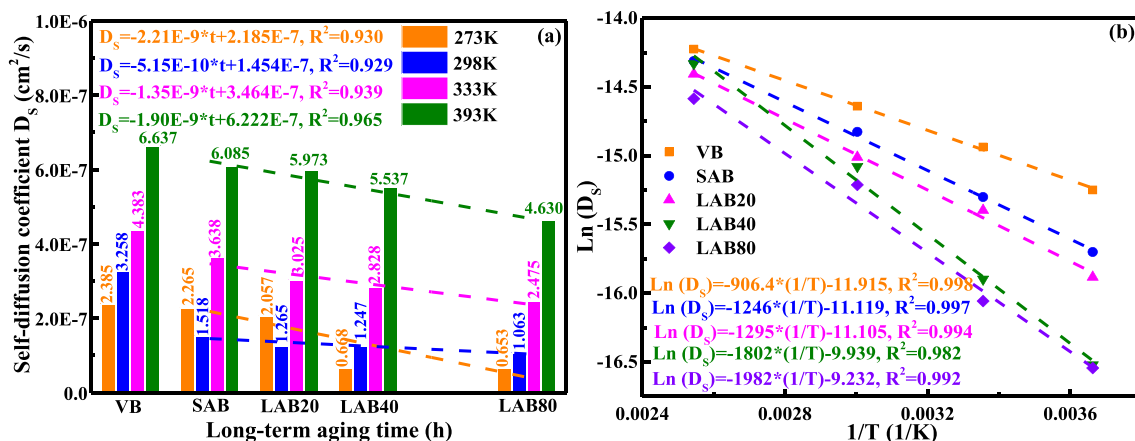


Fig. 9. Self-diffusion coefficient  $D_s$  of virgin and aged bitumen.

on the FFVR order of BORB, NORB, and AORB binders, strongly dependent on temperature and RA dosage. On the whole, BORB and NORB have a higher FFVR than AORB at low (273 K and 298 K) and high temperatures (393 K).

In addition, the aging effect on FFV values of rejuvenated bitumen is illustrated in Fig. 8. As the aging degree deepens, the FFV values decrease gradually, showing more difficult for recycling agents (RAs) to create new free volumes in a more aged bitumen. Interestingly, the variation trend of FFV and long-term aging time  $t$  of rejuvenate bitumen depends on the RA type. For BORB, NORB, and AORB, their FFV values decline exponentially as the aging time prolongs, while the FFV

parameter of the EORB binder shows a linear decreasing trend. Based on MD results in our previous work [27], the EO has a low molecular weight and polarity, and high molecular mobility. The low intermolecular interaction between EO and aged bitumen as well as high molecular movement contribute to a large free volume ratio in EORB. For other RAs, the increment in aging degree of bitumen enhances the intermolecular interactions between RAs with polar functional groups (bio-oil and aromatic-oil) and weakens their functions on enlarging the free volume. Meanwhile, the insufficient molecular mobility of naphthenic-oil molecules and the high molecular compactness of aged bitumen molecules both reduce the FFV value of NORB binder.



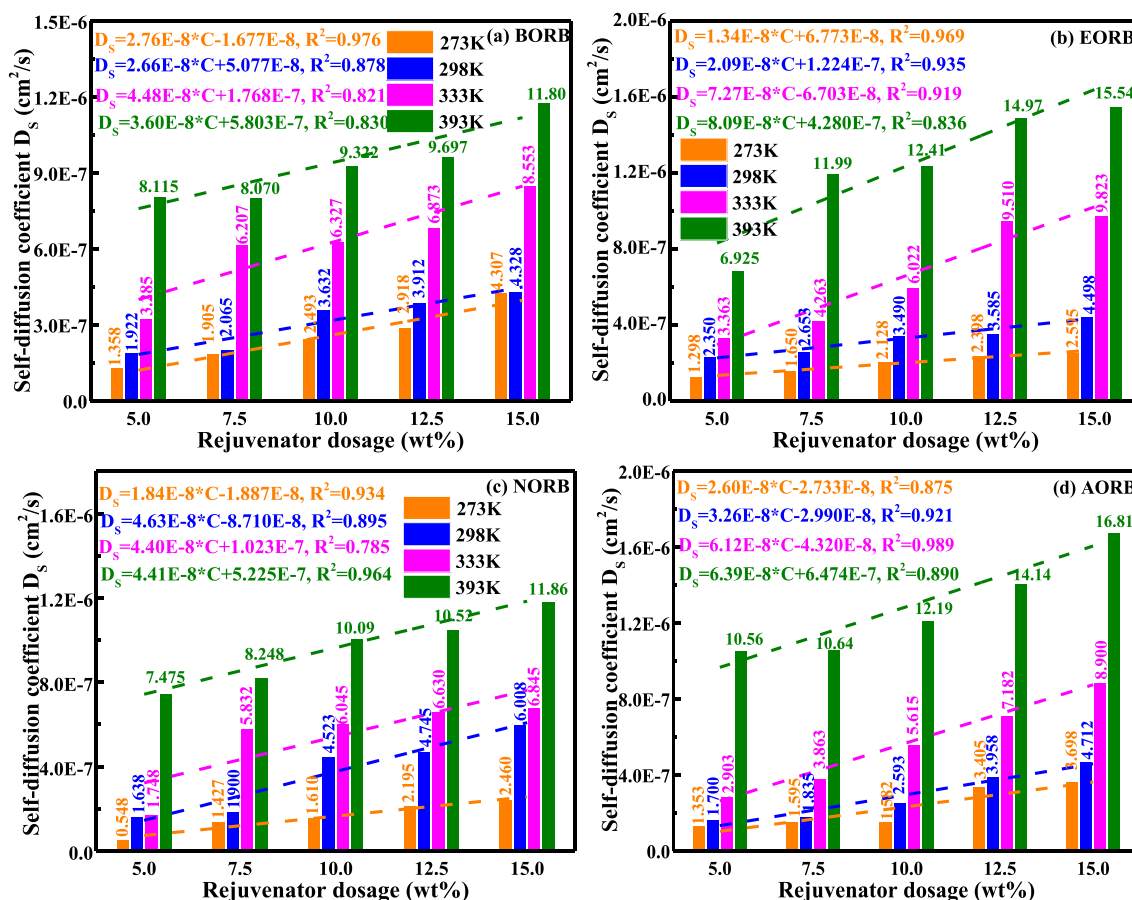


Fig. 10. Self-diffusion coefficient  $D_s$  values of rejuvenated bitumen.

## 5.2. Dynamic property of rejuvenated bitumen

### 5.2.1. Self-diffusion coefficient $D_s$

Fig. 9 illustrates the  $D_s$  values of virgin and aged bitumen as a function of long-term aging time and temperature. The  $D_s$  values for bitumen display a consistent decline as the aging time continues to extend, signifying that the aging process significantly diminishes the molecular mobility of bitumen molecules. Moreover, the increment in temperature significantly enlarges the  $D_s$  values of virgin and aged bitumen. For instance, when the temperature rises from 273 K to 298 K, 333 K, and 393 K, the  $D_s$  values of LAB40 aged bitumen increase by 0.87, 3.23, and 7.29 times, respectively. Additionally, temperature also affects the dependence level of the  $D_s$  value on aging time, more significant at high temperatures. The temperature sensitivity is evaluated by drawing the  $\ln(D_s) - (1/T)$ , shown in Fig. 9(b). The  $\ln(D_s)$  values correct well with  $(1/T)$  based on the high  $R^2$  values. From absolute slope values, the sensitivity level of  $\ln(D_s)$  value of bitumen to  $(1/T)$  change is more obvious as the aging level deepens.

The  $D_s$  values of various rejuvenated binders are displayed in Fig. 10, considering the influence of recycling agent (RA) type, dosage, and temperature. Regardless of RA type and temperature, the  $D_s$  values of all rejuvenated bitumen enlarge linearly as the RA dosage increases, which is converse to the aging effect. It suggests that all RAs play a positive role in restoring and improving the molecular motion capacity of aged bitumen. Meanwhile, the  $D_s$ -C curves of rejuvenated bitumen differ due to the difference in RA type and temperature. All  $D_s$  values of rejuvenated binders enlarge significantly as the temperature rises, especially when the temperature exceeds 298 K. Further, the temperature also affects the sensitivity level of  $D_s$  values to RA dosage, especially at high temperatures. Interestingly, the effects of RA type on  $D_s$  values of rejuvenated bitumen are inconsistent under variable temperatures and RA

dosages. Similar to the FFV parameter, the coupled effects of RA type, dosage, and temperature on the  $D_s$  values of rejuvenated bitumen are complex and interactive.

The  $D_s$ -based rejuvenation percentage DR values of rejuvenated bitumen are calculated for quantitatively assessing the rejuvenation efficiency of different recycling agents (RAs) on the dynamic behavior of aged bitumen (displayed in Fig. 11). All DR values of rejuvenated bitumen exhibit a linear and positive correlation with recycling agent (RA) dosage, indicating high RA dosage would promote the recovery and enhancement of molecular mobility of aged bitumen molecules. Moreover, the DR values become larger as the temperature rises. For all rejuvenated bitumen, the DR ranges at 273 K, 298 K, 333 K, and 393 K are 0–220 %, 0–250 %, 0–500 %, and 140–1600 %. It means a small RA dosage would result in a huge rejuvenation percentage at high temperatures (333 K and 393 K). The magnitude of DR values of rejuvenated bitumen is significantly affected by temperature and RA dosage. Thus, it is necessary to mention the simulation temperature and RA dosage when we plan to rank the rejuvenation efficiency of various RAs on restoring the dynamic property of aged bitumen.

### 5.2.2. Influence of aging degree on dynamic property

From Fig. 12, the corresponding self-diffusion coefficient  $D_s$  values of rejuvenated binders are strongly affected by the aging degree of bitumen. As the long-term aging time extends from 20 h to 40 h and 80 h, the  $D_s$  values of rejuvenated bitumen decline exponentially. The robust intermolecular bonds among highly aged bitumen molecules impede the molecular mobility of bitumen, consequently diminishing the stress relaxation capability of rejuvenated binders in low-temperature conditions. However, there is no explicit conclusion drawn regarding the effect of RA type on the variation trend of  $D_s$ -t curves of rejuvenated binders due to the difference in intermolecular

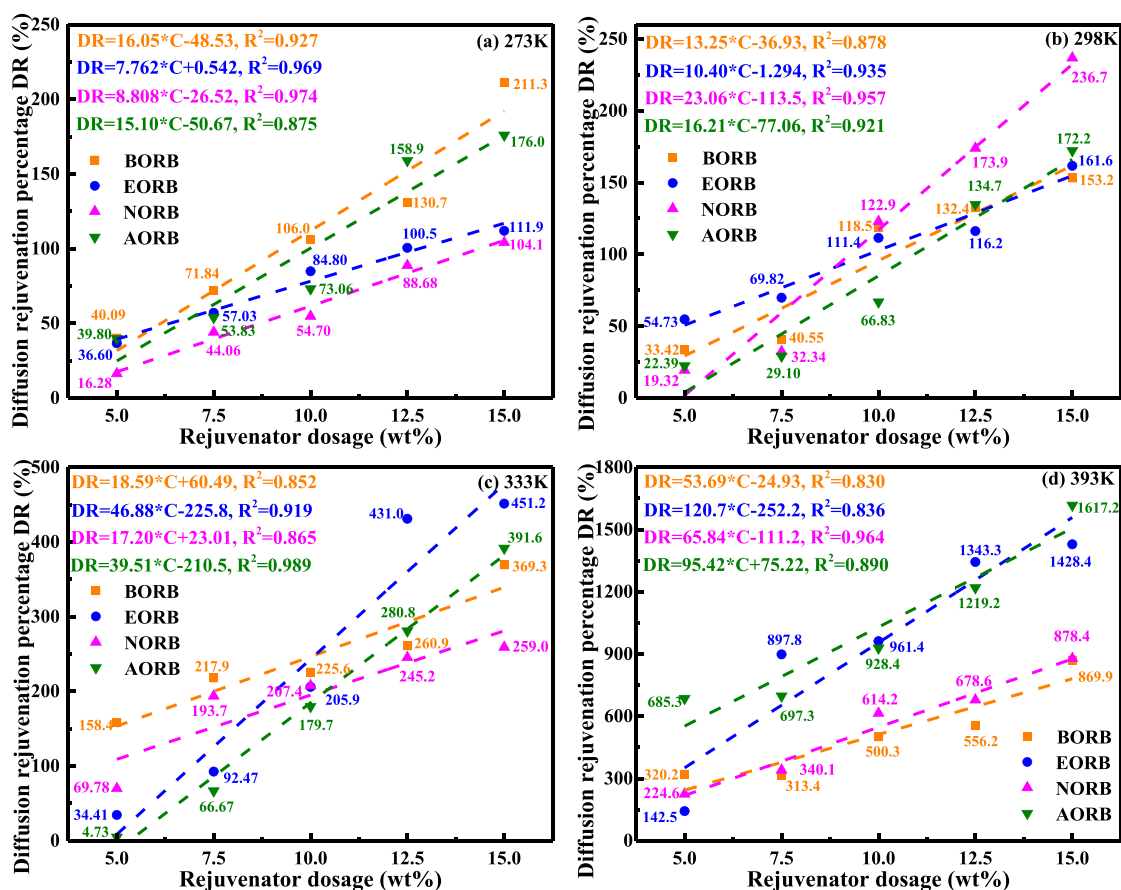


Fig. 11. Diffusion-based rejuvenation percentage DR of rejuvenated bitumen.

interactions between RAs and aged bitumen with variable aging levels.

It is noticed that the aging level also affects the temperature sensitivity of self-diffusion coefficient  $D_s$  values of rejuvenated bitumen. The  $\ln(D_s) - 1/T$  curves of rejuvenated bitumen with variable aging degrees and recycling agent (RA) types are plotted in Fig. 13. For BORB, EORB, and AORB binders, the increment in aging degree results in the reduction of temperature sensitivity of their  $D_s$  values. Besides, the NORB binder shows the opposite variation trend of temperature sensitivity versus aging level. Thus, the aging effect on temperature susceptibility of the  $D_s$  parameter of rejuvenated is dependent on the RA type. Table 4 lists the corresponding activation energy  $E_D$  and pre-exponential factor  $A$  of rejuvenated binders. The  $E_D$  and  $A$  values of BORB, EORB, and AORB binders both decrease as the aging degree deepens, whereas the  $E_D$  and  $A$  of NORB increase gradually. When the aging levels of bitumen are LAB20 and LAB80, the AORB binder exhibits the largest  $E_D$  value, followed by BORB, while EORB and NORB show similar and lower  $E_D$  values. This implies that the aromatic-oil exhibits the least improvement in restoring the self-diffusion capability of aged bitumen molecules. Interestingly, the AORB shows the lowest  $E_D$  value when the aging level is LAB80. It seems that the aromatic-oil is more effective in improving the molecular mobility of severely-aged bitumen. This could be attributed to the potential advantage of aromatic-oil molecules in breaking down molecular clusters and partially rejuvenating the colloidal structure of aged bitumen, although further evidence is required, including additional structural parameters for rejuvenated bitumen models.

### 5.3. Glass transition temperature of rejuvenated bitumen

Typically, the  $T_g$  value is established by identifying the temperature at which various thermodynamic properties, such as heat capacity, heat flow, and density, exhibit a significant change in sensitivity. In this

thesis, the  $T_g$  values of the virgin, aged, and rejuvenated binders are determined based on the variation curves of non-bond energy ( $E_N$ ) and free volume (FV) versus temperatures owing to their high-temperature sensitivity. Fig. 14 displays the  $E_N - T$  and FV-T curves of virgin and aged bitumen. As the increase in simulation temperature, the non-bond energy and free volume enlarge linearly. Their temperature sensitivity is dependent on the temperature region, and turning points in  $E_N - T$  and FV-T curves are observed as the glass transition temperatures. The slopes of  $E_N$  and FV values grow more pronounced after these turning points because bitumen molecules transition from the glassy (solid) state to the rubbery (viscoelastic solid) state. The correlation curves within two temperature regions are built separately to determine the  $T_g$  values. From the  $E_N - T$  curves, the predicted  $T_g$  values of VB, SAB, LAB20, LAB40, and LAB80 are 264.51 K, 272.37 K, 287.08 K, 311.85 K, and 331.34 K, respectively. Meanwhile, the  $T_g$  results from FV-T curves are 279.07 K, 280.21 K, 287.23 K, 316.11 K, and 340.61 K. It is concluded that the  $T_g$  values derived from  $E_N - T$  and FV-T curves are similar, and the former is slightly lower than the latter.

Fig. 15 shows the DSC curves of virgin and aged bitumen to measure their experimental  $T_g$  values. The heat flow variation was detected, and the glass transition temperatures ( $T_{g-onset}$ ,  $T_g$ , and  $T_{g-end}$ ) are also presented. The heat flow increases gradually as the temperature rises. For all bitumen samples, the  $T_g$  parameter is determined by monitoring the turning point where the variation rate of heat flow versus temperature changes significantly. Only one  $T_g$  point with the  $T_{g-onset}$  and  $T_{g-end}$  values is observed for virgin and aged bitumen, also marked in DSC curves. As the aging degree deepens, the  $T_g$  value of bitumen enlarges dramatically. The reason is that oxidation aging increases the polarity, molecular weight, and intermolecular force of bitumen molecules. More energy is required to surmount the external and self-constraints for molecular motion. Table 5 summarizes the measured and predicted  $T_g$

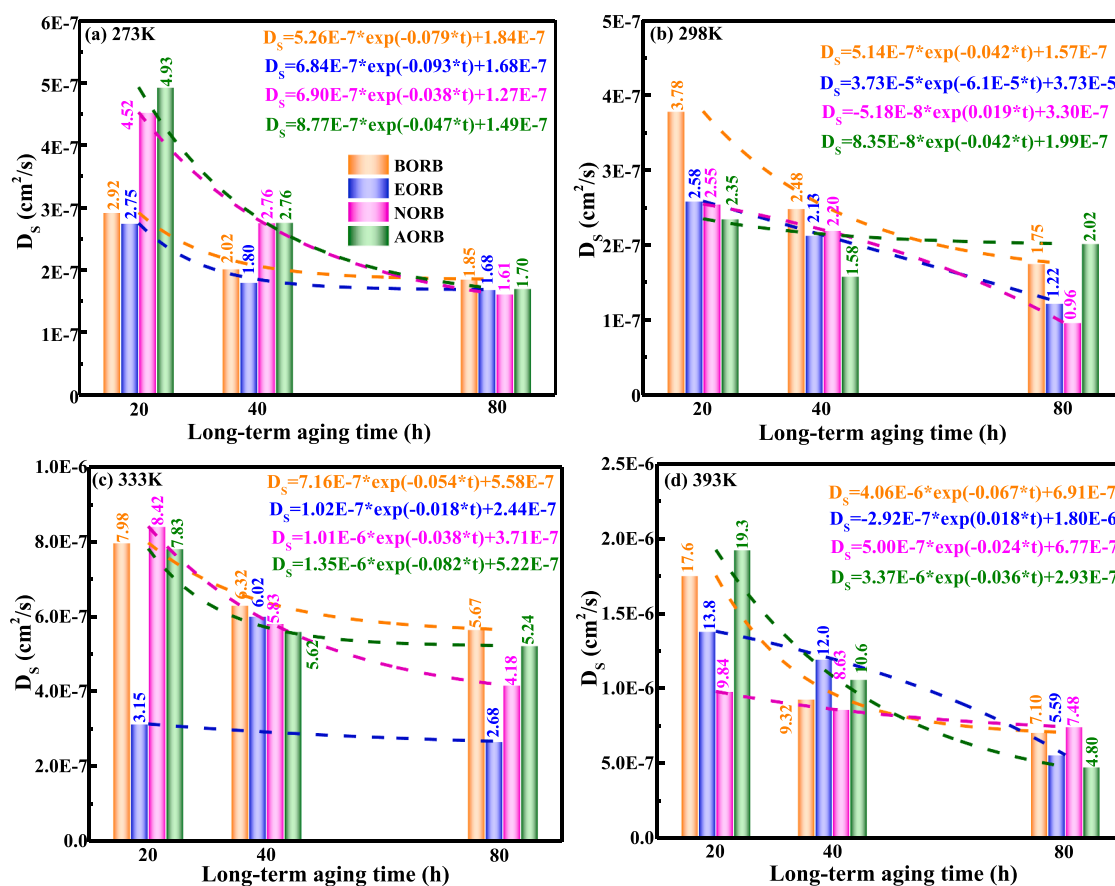


Fig. 12. Influence of aging time on  $D_s$  values of rejuvenated bitumen.

values of virgin and aged bitumen. The testing temperature increased from room temperature to 160 °C with an increment rate of 20 °C/min to completely relax the bitumen or recycling agent molecules. Afterward, the testing temperature declined gradually to 70 °C at 10 °C/min to determine the  $T_g$  point based on the heat flow-temperature curve [24,28]. It is denoted that there is a certain gap between MD simulation outputs and experimental results. The predicted  $T_g$  values are higher than the DSC results.

The  $E_N$ -T curves of rejuvenated bitumen with variable RA types and dosages are shown in Fig. 16. Regardless of temperature range, the non-bond energy  $E_N$  value of rejuvenated bitumen declines as a function of RA dosage. The correlation curves are built for determining the  $T_g$  values of rejuvenated bitumen, and the corresponding equations are listed in Table 6. It should be mentioned that the  $T_g$  determination process in FV-T curves is the same as in  $E_N$ -T curves, and thus the results are omitted here. Based on the  $R^2$  values, it is found that the non-bond energy correlates with temperature well. The predicted  $T_g$  values of virgin and aged bitumen are plotted in Fig. 17 based on non-bond energy and free volume. The  $T_g$  parameter shows a linear increasing trend as a function of long-term aging time. The FV-based  $T_g$  value is larger and more sensitive to long-term aging time than the  $E_N$ -based  $T_g$  value. Moreover, the  $T_g$  value of aged bitumen with variable aging levels can be forecasted using  $T_g$ -t correlation functions.

The glass transition temperature  $T_g$  values of rejuvenated bitumen with different recycling agent (RA) types and dosages are shown in Fig. 18. Regardless of RA type, the  $T_g$  values of rejuvenated bitumen reduce gradually as the RA dosage increases. This indicates that the inclusion of recycling agents (RAs) can substantially reinstate the  $T_g$  parameter, consequently enhancing the low-temperature performance of aged bitumen. When the RA dosage is the same, the order of  $T_g$  values for rejuvenated bitumen is BORB < EORB < NORB < AORB. This

elucidates the reason behind the superior low-temperature performance observed in bio-oil rejuvenated bitumen, with engine-oil, naphthenic-oil, and aromatic-oil rejuvenated binders following in decreasing order of performance. All  $T_g$  values of rejuvenated binders derived from non-bond energy show an exponentially decreasing trend versus RA content. Regarding the  $T_g$  values derived from the free volume, the BORB and AORB binders have an exponential trend, while the EORB and NORB show a linear correlation. Meanwhile, the FV-based  $T_g$  values of BORB and EORB are all higher than the  $E_N$ -based  $T_g$ , which depends on RA dosage for NORB and AORB cases.

To quantitatively evaluate the rejuvenation effectiveness of RAs, the  $T_g$ -based rejuvenation percentages  $T_gR$  values of rejuvenated bitumen are calculated and shown in Fig. 19. Due to the positive effect of RAs on  $T_g$  recovery, all  $T_gR$  values of rejuvenated bitumen increase as the RA dosage rises. However, the variation trend of  $T_gR$ -C curves depends on the determination way of the  $T_g$  parameter. For  $E_N$ -based  $T_g$ , the corresponding  $T_gR$  shows an exponential trend versus RA dosage, while the  $T_gR$  based on FV linearly correlates with RA dosage. Furthermore, all  $E_N$ -based  $T_gR$  of rejuvenated bitumen is lower than 100 %, indicating that the addition of RAs even with the dosage of 15 % fails to completely restore the  $T_g$  value of aged bitumen to the virgin bitumen level. For FV-based  $T_gR$  values, the same finding is observed, except for the BORB sample with 15 % bio-oil. Interestingly, the magnitude of  $E_N$ -based  $T_gR$  for rejuvenated bitumen (BORB > EORB > NORB > AORB) is independent of RA dosage, while it is difficult to rank the FV-based  $T_gR$  values of EORB and NORB binders. Thus, the  $E_N$ -based  $T_g$  index is more appropriate to be an effective indicator for rejuvenation efficiency evaluation than the FV-based  $T_g$  index.

The effect of aging degree on the  $T_g$  values of rejuvenated bitumen is also investigated, and the results are shown in Fig. 20. All  $T_g$  values of rejuvenated binders tend to increase significantly as the long-term aging

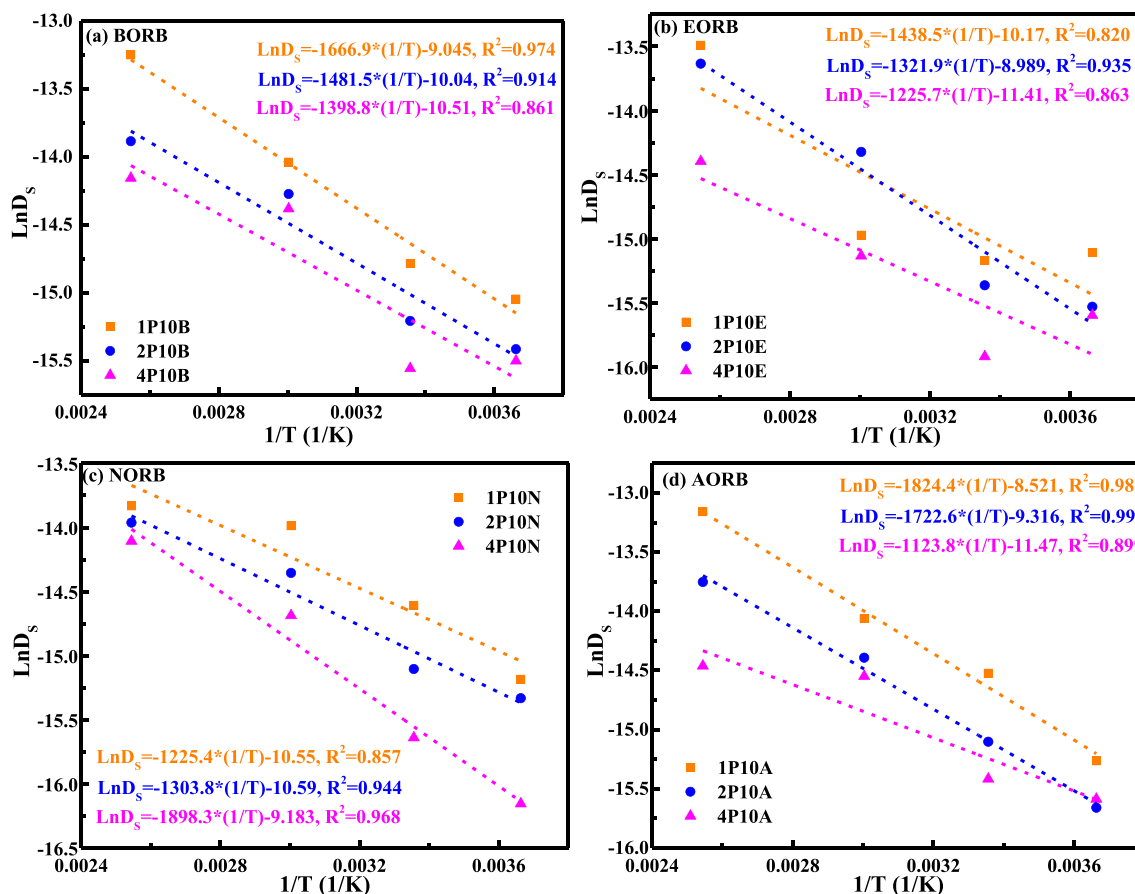


Fig. 13. Influence of aging time on  $\ln(D_s)$ - $1/T$  curves of rejuvenated bitumen.

Table 4

Influence of aging level on  $E_D$  and A parameters.

Samples	$E_D$ (J/mol)	A	Samples	$E_D$ (J/mol)	A
1P10B	13858.6	1.180E-4	1P10N	10188.0	2.619E-5
2P10B	12317.2	4.362E-5	2P10N	10839.8	2.517E-5
4P10B	11629.6	2.726E-5	4P10N	15782.5	1.028E-4
1P10E	11959.7	3.830E-5	1P10A	15168.1	1.992E-4
2P10E	11047.3	1.248E-5	2P10A	14321.7	8.997E-5
4P10E	10190.5	1.108E-5	4P10A	9343.3	1.044E-5

time of bitumen deepens from 20 to 40 and 80 h. It is noticed that most  $T_g$  values of rejuvenated bitumen show an exponentially positive connection with long-term aging time, except for the FV-based  $T_g$  of NORB and AORB binders. The  $E_N$ -based  $T_g$  ranking of rejuvenated bitumen (BORB < EORB < NORB < AORB) remains constant, while the FV-based  $T_g$  order depends on the aging level of bitumen. Eventually, the  $E_N$ -based  $T_g$  is recommended as an evaluation index and will be connected with macroscale low-temperature indicators. One intriguing observation is that the impact of aging on the  $T_g$  value of bitumen diminishes as the aging degree intensifies, whereas the influence of the RA dosage on  $T_g$  becomes increasingly pronounced with higher levels of RA content.

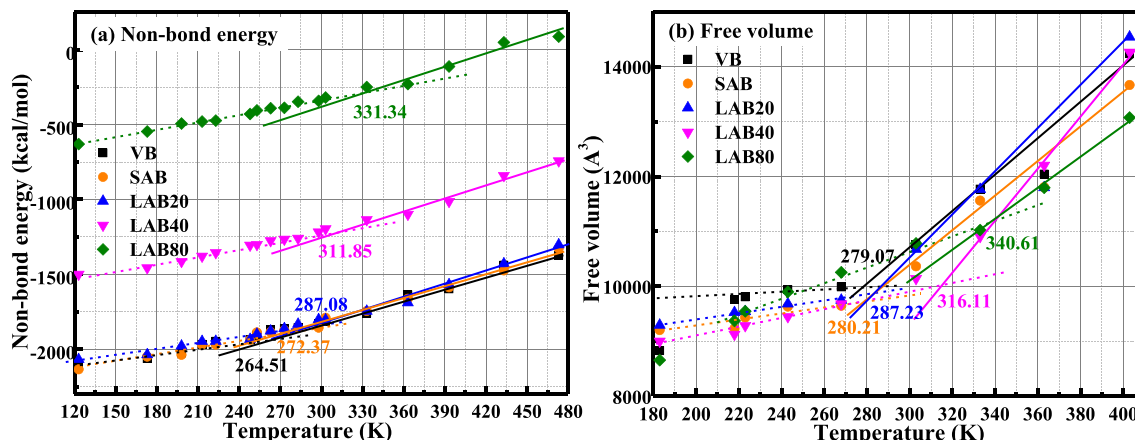


Fig. 14. The  $E_N$ - $T$  and  $V_F$ - $T$  curves of virgin and aged bitumen.

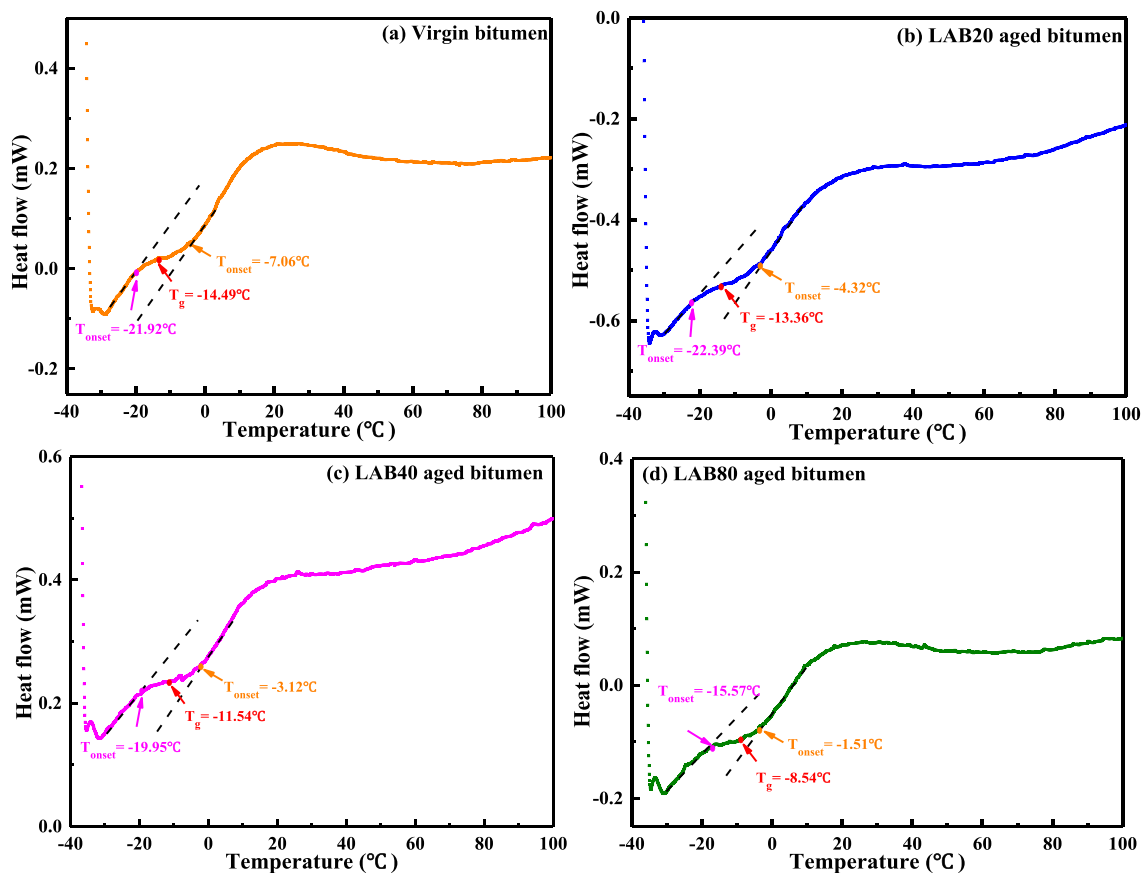


Fig. 15. The DSC curves of virgin and aged bitumen.

Table 5

$T_g$  values of virgin and aged bitumen from experiment and MD simulation.

Items	Bitumen	VB	LAB20	LAB40	LAB80
Experiment	$T_{g\text{-onset}}$ (°C)	-21.92	-22.39	-19.95	-15.57
	$T_{g\text{-end}}$ (°C)	-7.06	-4.32	-3.12	-1.51
	$T_g$ (°C)	-14.49	-13.36	-11.54	-8.54
MD simulation ( $E_N$ -T)	$T_g$ (°C)	-8.64	13.93	38.70	58.19
MD simulation (FV-T)	$T_g$ (°C)	5.92	14.10	42.98	67.48

#### 5.4. Surface free energy and work of cohesion of rejuvenated bitumen

The surface free energy ( $\gamma$ ) values of virgin, aged, and rejuvenated bitumen models are predicted from MD simulation to investigate the rejuvenation efficiency of various RAs on the cohesive property of aged bitumen. The  $\gamma$  results at 273 K are summarized in Fig. 21. As the long-term aging prolongs, the surface free energy of bitumen declines dramatically, indicating that the cohesive cracking potential of aged bitumen becomes easier. Meanwhile, the correlation between  $\gamma$  and aging time  $t$  is obtained to forecast the  $\gamma$  value of aged bitumen with variable aging levels.

The variation trends of  $\gamma$  curves as a function of RA dosage of different rejuvenated binders are illustrated in Fig. 21(b). Regardless of RA type, the  $\gamma$  index tends to increase linearly versus RA content. It suggests that high RA dosage promotes the enhancement of  $\gamma$  and cracking resistance of rejuvenated bitumen. Moreover, the rejuvenation effect on the  $\gamma$  index depends on the RA type. When the RA dosage is the same, the magnitude of  $\gamma$  values for rejuvenated binders is BORB > EORB > NORB > AORB. This aligns with the experimental fatigue findings, demonstrating that the BO yields the most substantial improvement in the fatigue performance of aged bitumen, followed by EO and NO, whereas the AO displays the least rejuvenating effect. It is

expected that the  $\gamma$  parameter connects well with the critical fatigue indicators measured from experiments. The sensitivity of  $\gamma$  value of BORB to RA dosage is the largest, followed by EORB, NORB, and AORB binders. Fig. 21(c) displays the  $\gamma$  values of rejuvenated bitumen with the same RA dosage of 10 wt% as a function of the aging degree. The research indicates that as the aging level increases, the  $\gamma$  values of rejuvenated bitumen decrease exponentially, underscoring the detrimental impact of aging on the cohesive cracking resistance of rejuvenated bitumen. Notably, the order of  $\gamma$  values (BORB > EORB > NORB > AORB) remains consistent regardless of the bitumen's aging level. Table 7 lists the calculated work of cohesion  $W_{aa}$  values of virgin, aged, and rejuvenated bitumen based on Eq.5. The  $W_{aa}$  value is twice as much as  $\gamma$ , and thus it shows the same variation trend as the  $\gamma$  parameter.

The  $\gamma$ -based rejuvenation efficiency values  $\gamma R$  of rejuvenated bitumen are calculated following Eq.6, and the results are demonstrated in Fig. 22. The  $\gamma R$  values of rejuvenated bitumen show a linearly increasing trend as the RA dosage rises with an increasing slope of 4.314, 1.438, 1.353, and 1.033 for BORB, EORB, NORB, and AORB binders, respectively. It manifests that the bio-oil exhibits the greatest benefit in improving the cohesive cracking resistance of aged bitumen. With the long-term aging time  $t$  prolongs, the  $\gamma R$  values of rejuvenated bitumen decline gradually. However, the variation trends of  $\gamma R$ - $t$  curves of rejuvenated bitumen depend on the RA type. For BORB and EORB binders, the  $\gamma R$ - $t$  curves have an exponentially decreasing trend, while the  $\gamma R$  values of NORB and AORB binders reduce linearly as an increase in the aging degree of bitumen. The  $\gamma R$  values of rejuvenated bitumen are in the region of 20–180 %, depending on the RA type/dosage and aging degree. Meanwhile, the magnitude of  $\gamma R$  (BORB > EORB > NORB > AORB) is independent of RA dosage and aging level of bitumen. Thus, the surface free energy  $\gamma$  is an effective index to evaluate the rejuvenation efficiency of various RAs on the cohesive cracking potential of aged bitumen.



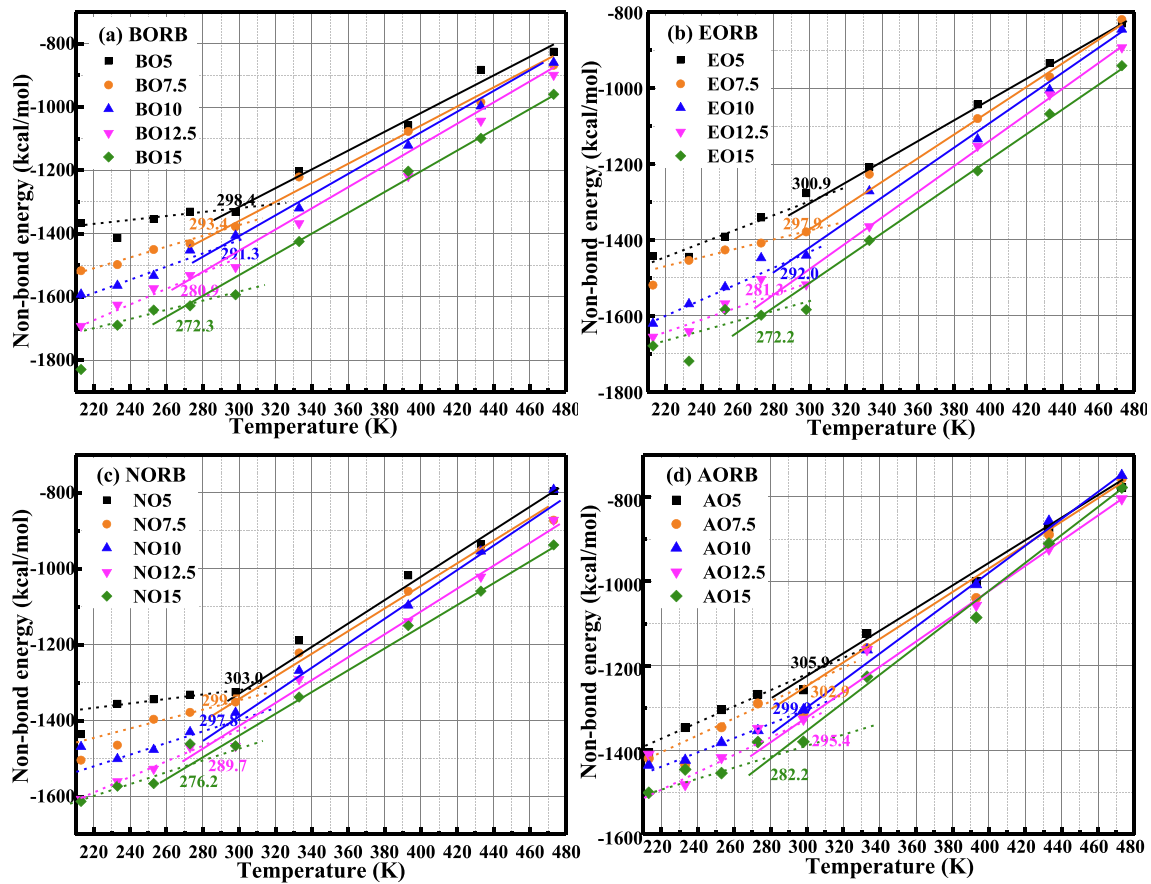


Fig. 16. The  $E_N$ -T curves of rejuvenated bitumen.

Table 6  
Correlation equation parameters in  $E_N$ -T curves of rejuvenated bitumen.

Samples	Equation (1)			Equation (2)		
	Slope	Intercept	R <sup>2</sup>	Slope	Intercept	R <sup>2</sup>
BO5	0.4586	-1464.72	0.915	2.7973	-2162.69	0.995
BO7.5	1.6473	-1873.77	0.975	2.9800	-2264.77	0.993
BO10	1.4734	-1906.62	0.998	2.9595	-2339.56	0.999
BO12.5	2.6753	-2255.74	0.984	3.2187	-2408.38	0.997
BO15	1.4025	-2008.92	0.932	3.3370	-2535.67	0.999
EO5	1.6327	-1793.91	0.933	2.6753	-2107.65	0.999
EO7.5	1.1285	-1793.91	0.933	2.6753	-2107.65	0.999
EO10	2.0862	-2058.50	0.991	3.4204	-2448.11	0.997
EO12.5	1.7111	-2021.92	0.905	3.3575	-2484.97	0.999
EO15	1.1624	-1924.22	0.957	3.3181	-2511.09	0.998
NO5	0.4916	-1469.06	0.957	2.9290	-2207.65	0.993
NO7.5	1.0156	-1654.37	0.995	2.9525	-2234.82	0.998
NO10	1.9280	-1956.24	0.981	3.1016	-2304.34	0.997
NO12.5	2.2100	-2078.21	0.985	2.9091	-2280.70	0.994
NO15	1.6770	-1972.52	0.943	2.8177	-2287.62	0.999
AO5	1.9778	-1806.89	0.996	2.5107	-1969.92	0.989
AO7.5	2.1237	-1875.00	0.974	2.8854	-2105.77	0.995
AO10	1.8021	-1842.45	0.994	3.2033	-2262.70	0.997
AO12.5	2.3266	-2016.72	0.972	3.0196	-2221.42	0.999
AO15	-1.4257	-1808.46	0.981	3.1345	-2290.74	0.995

6. Critical low-temperature and fatigue properties from experiments

The critical low-temperature and fatigue parameters of rejuvenated binders are shown in Table 8. The long-term aging significantly enhances the  $\tau_{50\%}$ ,  $t_{25\%}$ , A, FFT, E, and  $C_{500}$  values of bitumen, and reduces the  $N_{f5}$  and  $\epsilon_{sr}$  parameters. It manifests that long-term aging remarkably weakens the relaxation capacity and fatigue resistance of bitumen. The

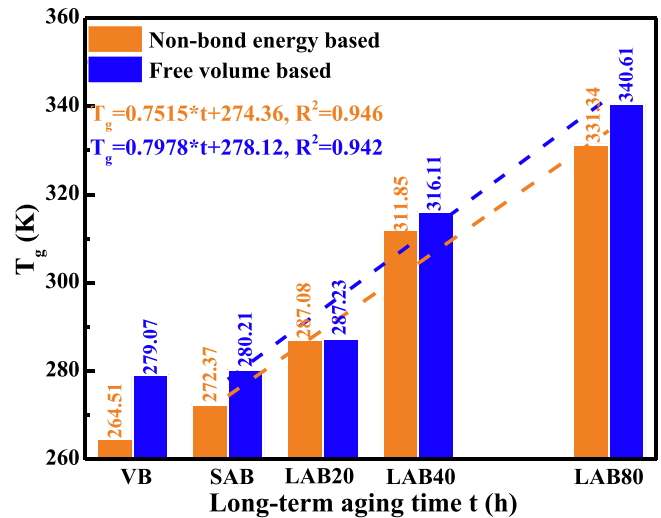
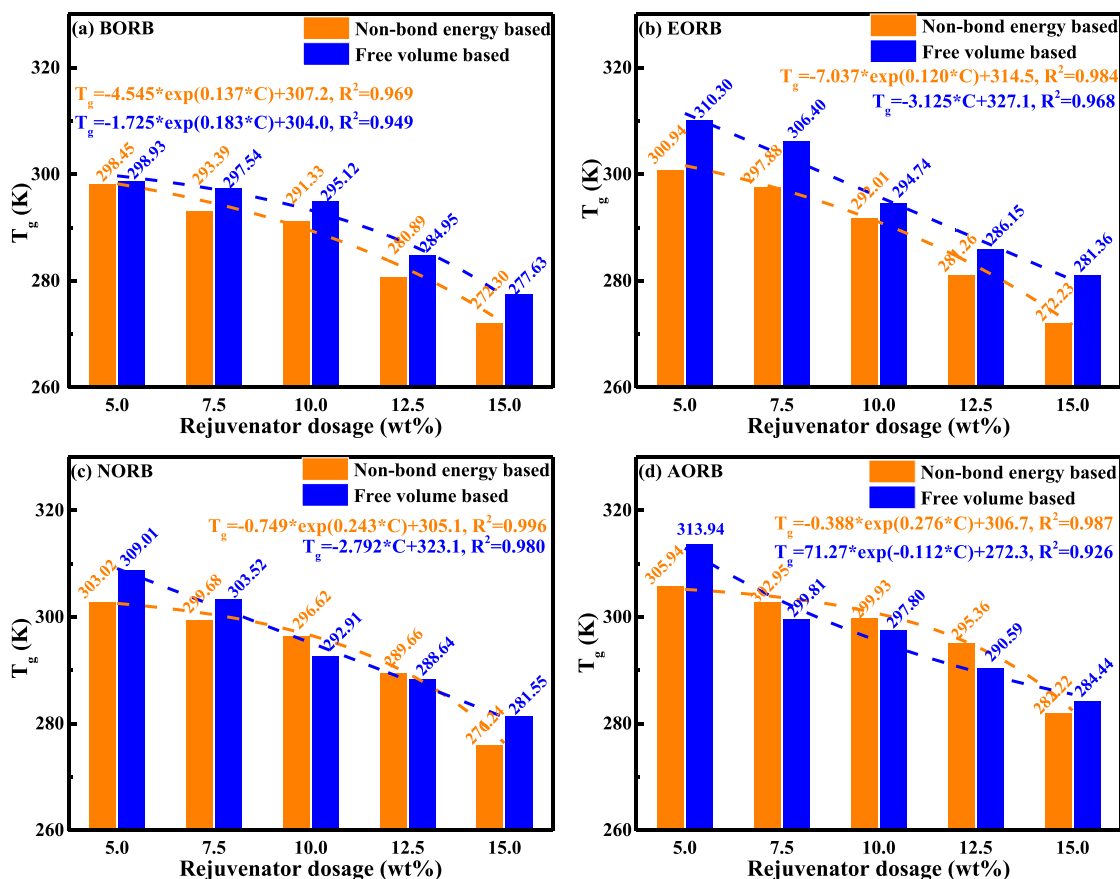
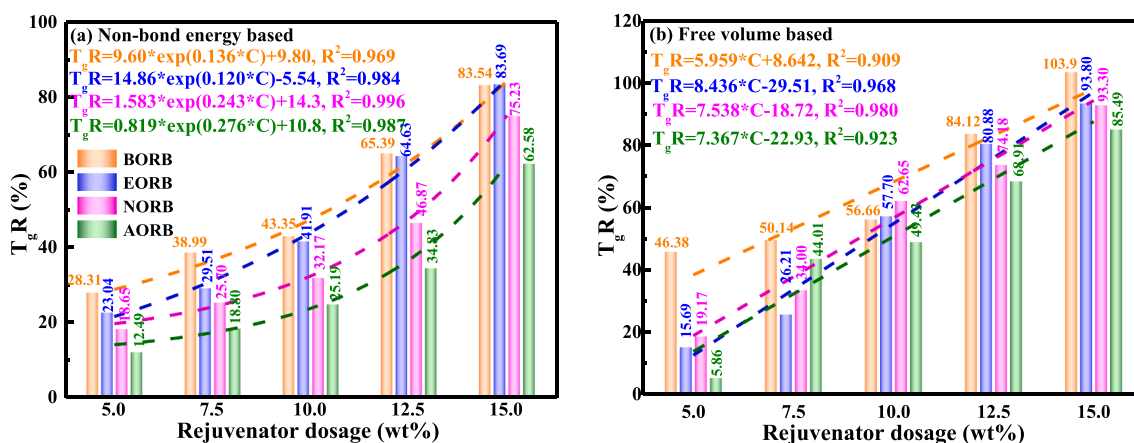


Fig. 17. The glass transition temperature  $T_g$  values of virgin and aged bitumen.

incorporation of RAs exhibits an opposite influence on these critical rheological parameters, and the rejuvenation effect becomes stronger as the RA dosage rises.

The crossover parameters, namely crossover modulus ( $G_c$ ) and crossover frequency ( $f_c$ ), along with the Glover-Rowe (G-R) index, have been identified as effective indicators to distinguish between softeners and rejuvenators [34,35]. In Fig. 23, the impact of aging and rejuvenation on  $G_c$ ,  $f_c$ , and G-R values of bitumen is illustrated. With increasing long-term aging, both  $Lg(f_c)$  and  $Lg(G_c)$  values exhibit a linear decrease,

Fig. 18. The glass transition temperature  $T_g$  of rejuvenated bitumen.Fig. 19. The  $T_g$ -based rejuvenation percentage  $T_gR$  of rejuvenated bitumen.

attributed to the enlarged size of asphaltene nanoaggregates and intermolecular interactions. Simultaneously, the G-R parameter experiences an exponential increase, particularly between 40 and 80 h of aging, aligning with previous findings that the binder's restoration capacity diminishes after 80 h, reaching its maximum aging limit [34].

The efficacy of rejuvenation on  $G_c$ ,  $f_c$ , and G-R values of aged bitumen is significantly influenced by the type and dosage of the recycling agent. All recycling agents can restore the  $f_c$  and G-R indices of aged bitumen, with efficiencies increasing alongside higher dosages. Notably, only aromatic-oil demonstrates a positive effect on recovering the crossover modulus of aged binder, indicating its role as a rejuvenator, while others function as softeners in restoring the molecular

conformation of aged bitumen. This is attributed to the polar aromatic motif in aromatic-oil, which can easily disrupt the asphaltene stack through  $\Pi$ - $\Pi$  stacking interactions [36].

The restoration efficiency of bio-oil and aromatic-oil on crossover frequency surpasses that of naphthenic-oil and engine-oil. Engine-oil exhibits the lowest efficiency on both  $G_c$  and  $f_c$ , while bio-oil demonstrates the highest potential for restoring the  $f_c$  index. Consequently, bio-oil and naphthenic-oil emerge as more efficient recycling agents compared to engine-oil. The polar ester functional group in bio-oil plays a role in weakening  $\Pi$ - $\Pi$  interactions between asphaltene sheets, distinguishing it from the less polar naphthenic-oil and saturated engine-oil [35]. However, despite its efficacy, bio-oil falls short of restoring the  $G_c$

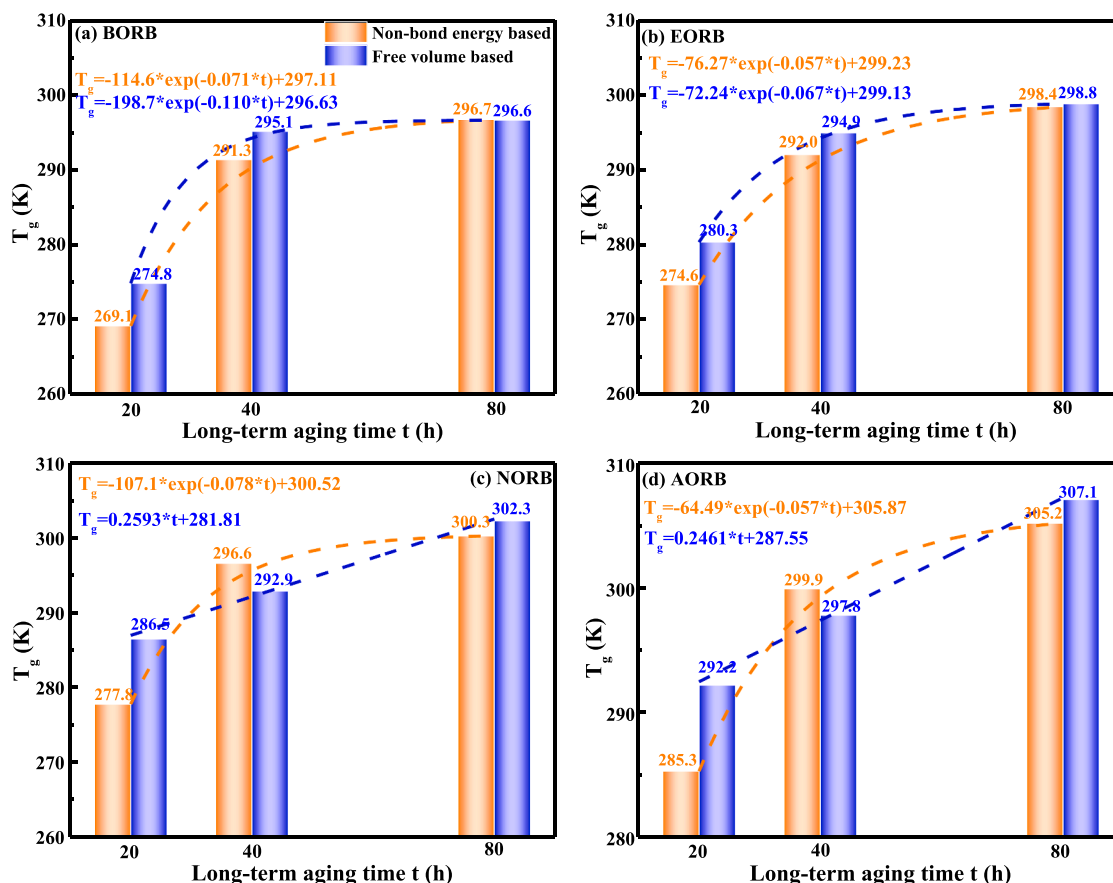
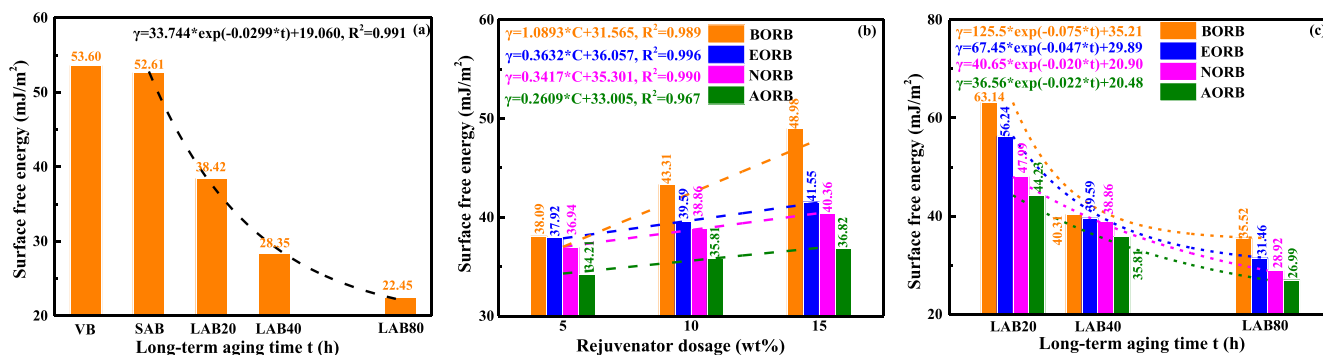
Fig. 20. Aging influence on  $T_g$  values of rejuvenated bitumen.Fig. 21. Surface free energy  $\gamma$  of the virgin, aged, and rejuvenated bitumen.

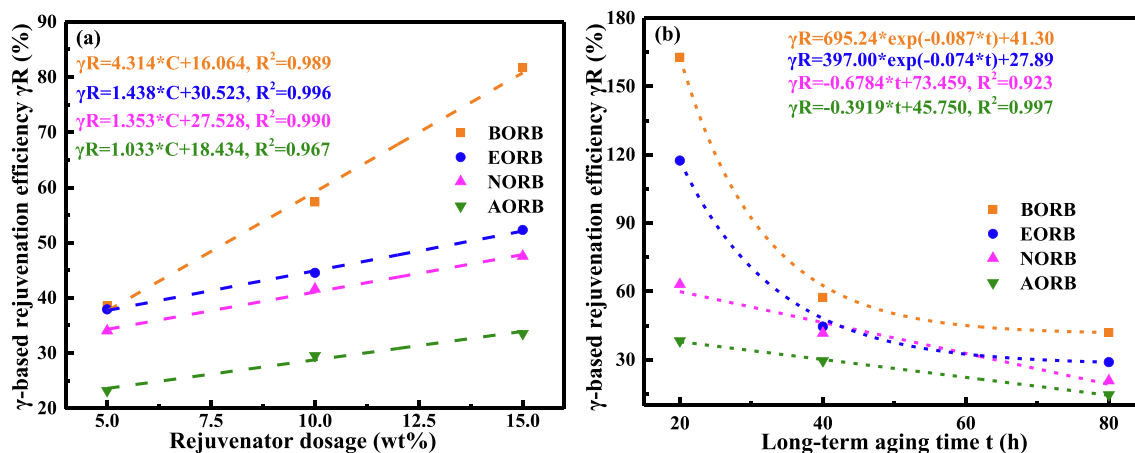
Table 7

Work of cohesion  $W_{aa}$  of the virgin, aged, and rejuvenated bitumen.

Samples	$W_{aa}$ (mJ/m <sup>2</sup> )	Samples	$W_{aa}$ (mJ/m <sup>2</sup> )	Samples	$W_{aa}$ (mJ/m <sup>2</sup> )
VB	107.20	SAB	105.22	LAB20	76.84
LAB40	56.70	LAB80	44.90	-	-
2P5B	76.17	2P5N	73.88	1P10B	126.28
2P10B	86.62	2P10N	77.71	1P10E	112.48
2P15B	97.96	2P15N	80.72	1P10N	95.98
2P5E	75.84	2P5A	68.42	1P10A	88.46
2P10E	79.18	2P10A	71.62	4P10B	71.03
2P15E	83.11	2P15A	73.64	4P10E	62.92
-	-	4P10N	57.83	4P10A	53.98

index compared to aromatic-oil.

Notably, all recycling agents can recover thermodynamic indices (FFV,  $D_s$ ,  $T_g$ , and  $\gamma$ ) of aged bitumen, yet most act as softeners rather than rejuvenators. Consequently, these thermodynamic indices reflect the restoration effect of recycling agents but do not distinguish between softeners and rejuvenators. To address this, it is crucial to explore their efficiency in disrupting asphaltene stacks and molecular conformation when selecting rejuvenators over softeners, as this strongly relates to the durability, aging, and moisture resistance of rejuvenated bitumen [35]. Fig. 23(f) reveals that softeners (bio-oil, engine-oil, and naphthenic-oil) exhibit better recovery efficiency on the G-R value of aged bitumen compared to the rejuvenator (aromatic-oil). This underscores that the addition of recycling agents, even softeners, can enhance the low-temperature anti-cracking performance of aged bitumen. Achieving both short-term and long-term rejuvenation efficiency necessitates a

Fig. 22.  $\gamma$ -based rejuvenation efficiency  $\gamma_R$  of rejuvenated bitumen.

**Table 8**  
Critical low-temperature and fatigue parameters of rejuvenated bitumen.

Samples	$\tau_{50s}$ (Pa)	$t_{25\%}$ (s)	A	FFT (°C)	$N_{15}$ (Cycles)	E (Pa)	$\varepsilon_{sr}$	$C_{500}$ (mm)	Gc (Pa)	$f_c$ (Hz)	G-R (kPa)
VB	16,029	1.35	190,140	12.75	426	1.336E7	0.077	0.462	1.98E7	65.74	5.29
SAB	24,841	1.87	232,486	15.47	341	1.460E7	0.073	0.449	1.23E7	15.61	15.5
LAB20	43,255	2.80	295,079	17.55	186	1.840E7	0.067	0.594	7.14E6	1.26	41.2
LAB40	72,493	5.05	397,272	27.77	167	2.600E7	0.045	0.819	4.76E6	0.17	70.02
LAB80	149,540	13.47	571,349	32.27	108	3.860E7	0.043	1.482	2.57E6	0.009	542.16
1P10B	1886	0.70	29,037	2.92	1091	2.214E6	0.116	0.202	4,703,876	38.48	1.16
1P10E	2586	0.97	36,101	4.11	866	2.737E6	0.125	0.240	2,956,785	10.73	1.54
1P10N	7930	1.15	60,642	7.07	845	4.065E6	0.116	0.267	3,931,818	8.98	3.55
1P10A	17,190	1.44	152,653	13.09	314	9.076E6	0.081	0.260	10,651,116	14.2	7.19
2P5B	19,277	1.95	139,159	12.18	534	9.158E6	0.104	0.403	3,239,710	1	15.74
2P7.5B	11,878	1.46	87,320						2,836,760	2	
2P10B	4977	1.08	45,070	4.84	1079	3.430E6	0.131	0.257	2,326,460	4	4.1
2P12.5B	3368	0.85	28,954						1,975,410	5.65	
2P15B	1715	0.83	17,303	-1.55	1492	1.600E6	0.154	0.191	1,778,650	11.3	0.7
2P5E	24,474	2.46	160,566	12.78	460	9.960E6	0.094	0.443	3,127,660	0.711	14.18
2P7.5E	13,868	1.98	96,990						1,927,790	0.711	
2P10E	9142	1.66	64,589	6.48	839	4.400E6	0.133	0.326	1,857,630	1.42	6.15
2P12.5E	5595	1.52	42,760						1,239,510	1.42	
2P15E	3827	1.27	31,941	1.05	1103	2.230E6	0.136	0.274	1,082,610	2	1.94
2P5N	26,678	2.47	180,136	13.72	415	1.130E7	0.087	0.480	3,503,520	0.711	14.25
2P7.5 N	16,238	1.99	106,168						2,440,030	1	
2P10N	11,143	1.66	81,369	8.27	684	5.520E6	0.103	0.352	2,644,640	2	6.29
2P12.5 N	7163	1.37	58,037						2,264,000	2.83	
2P15N	4023	1.24	41,992	3.92	894	3.050E6	0.146	0.270	2,046,430	4	1.83
2P5A	54,583	3.45	332,747	17.64	236	1.840E7	0.068	0.615	5,783,090	0.711	29.64
2P7.5A	42,813	2.74	286,674						5,723,340	1	
2P10A	33,692	2.23	249,641	15.58	277	1.350E7	0.075	0.517	7,633,560	2.83	12.27
2P12.5A	27,416	1.81	217,766						7,796,810	4	
2P15A	19,501	1.53	182,548	13.68	383	9.970E6	0.090	0.408	9,071,640	7.98	6.5
4P10B	18,115	2.51	98,824	9.41	688	7.310E6	0.112	0.390	933,592	0.091	38.71
4P10E	23,887	4.16	102,726	10.23	544	7.900E6	0.097	0.480	769,126	0.036	75.1
4P10N	33,692	4.57	148,344	12.79	534	1.070E7	0.087	0.512	965,671	0.033	119.92
4P10A	55,762	3.86	308,769	17.35	200	1.780E7	0.065	0.680	3,602,448	0.185	127.15

balance in chemical components and restoration of molecular conformation [36].

## 7. Potential connection exploration between thermodynamic and rheological parameters of rejuvenated bitumen

### 7.1. Low-temperature performance correlation

It is important to detect the potential connections between low-temperature critical indicators (shear stress  $\tau_{50s}$ , relaxation time  $t_{25\%}$ , and A) proposed in previous work [25] and thermodynamic properties (self-diffusion coefficient  $D_s$ , fractional free volume FFV, and glass transition temperature  $T_g$ ) predicted from MD simulations. The detailed

correlation curves and equations are summarized in Fig. 24.

As the self-diffusion coefficient  $D_s$  increases, all relaxation indicators ( $\tau_{50s}$ ,  $t_{25\%}$ , and A) tend to decrease exponentially. Moreover, the shear stress  $\tau_{50s}$  and relaxation time  $t_{25\%}$  values decline exponentially as a function of fractional free volume FFV, while the A index decreases linearly. This implies that elevated  $D_s$  and FFV values can effectively lower relaxation stress and duration, consequently enhancing the relaxation capabilities of bituminous materials. This observation aligns with the established understanding that molecular mobility and free volume are pivotal factors in material relaxation [21]. Additionally, the  $T_g$  index shows positive and exponential relationships with relaxation parameters, showing that the bitumen with a higher  $T_g$  value would prefer the worse relaxation performance at low temperatures.

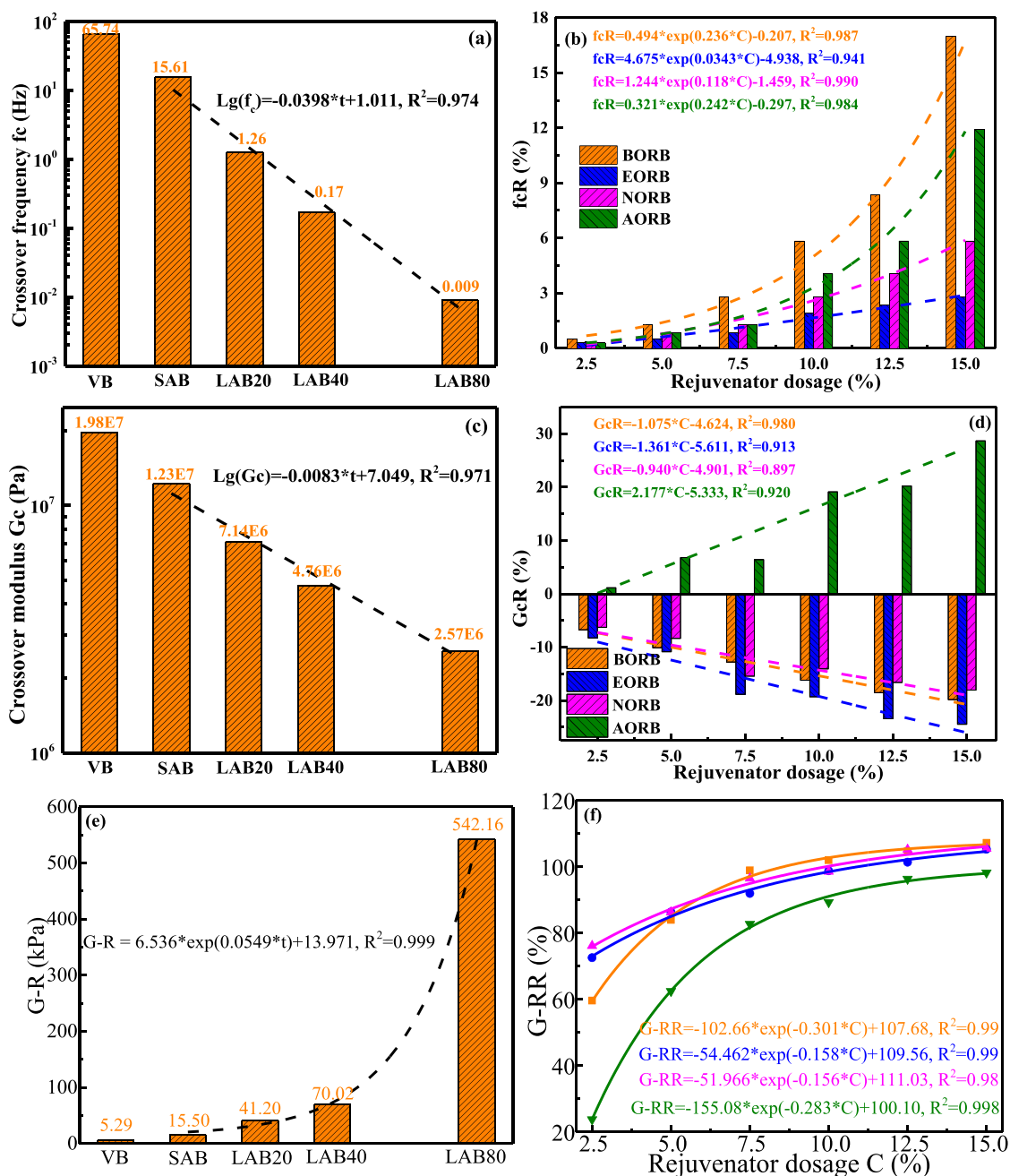


Fig. 23. Aging and rejuvenation effect on  $G_c$ ,  $f_c$ , and  $G-R$  parameters of bitumen.

Regarding the correlation degree, the  $R^2$  values of  $\tau_{50s}$ - $D_s$ ,  $t_{25\%}$ - $D_s$ , and  $A$ - $D_s$  curves are 0.3–0.5, showing the self-diffusion coefficient  $D_s$  parameter presents unsatisfactory connections with critical relaxation indicators. This is possibly due to the intricate nature of bitumen's relaxation behavior, where a molecule's diffusion capacity can impact but doesn't entirely dictate the material's relaxation characteristics [23]. On the contrary, the FFV parameter connects well with the  $\tau_{50s}$  and  $t_{25\%}$  indices based on the high correlation coefficient  $R^2$  values of 0.875 and 0.846, respectively. However, the association effect of the FFV- $A$  curve is poor with a low  $R^2$  of 0.560. Lastly, the  $R^2$  values of  $\tau_{50s}$ - $T_g$ ,  $t_{25\%}$ - $T_g$ , and  $A$ - $T_g$  curves are 0.850, 0.653, and 0.582, respectively.

Overall, the relaxation model parameter  $A$  fails to connect well with all thermodynamic parameters. Meanwhile, the shear stress  $\tau_{50s}$  shows greater connections with thermodynamic indices than the relaxation time  $t_{25\%}$ . On the other hand, the  $D_s$  have a lower association effect with critical relaxation indicators than the FFV and  $T_g$  indices. Furthermore,

the FFV parameter exhibits a greater correlation with  $\tau_{50s}$  and  $t_{25\%}$  than  $T_g$ . Therefore, it is recommended to predict the relaxation properties of different rejuvenated bitumen by the fractional free volume parameter from MD simulation. Eventually, the best correlation is the FFV- $\tau_{50s}$ , which can be adapted to evaluate the rejuvenation efficiency of various recycling agents on low-temperature relaxation behaviors of aged bitumen.

The interrelationships between crossover parameters ( $G_c$  and  $f_c$ ) and thermodynamic indices (FFV and  $T_g$ ) of virgin, aged, and various rejuvenated bitumen were investigated and depicted in Fig. 25. The analysis reveals a strong correlation between the  $f_c$  values of all bitumen binders and both FFV and  $T_g$  indices. The  $f_c$  index exhibits an exponential increase with rising FFV, while it shows an exponential decrease with increasing  $T_g$ . Consequently, the  $f_c$  value of bitumen can be predicted based on MD simulations using FFV and  $T_g$  indices. In terms of the  $G_c$  index, its potential association with thermodynamic parameters is



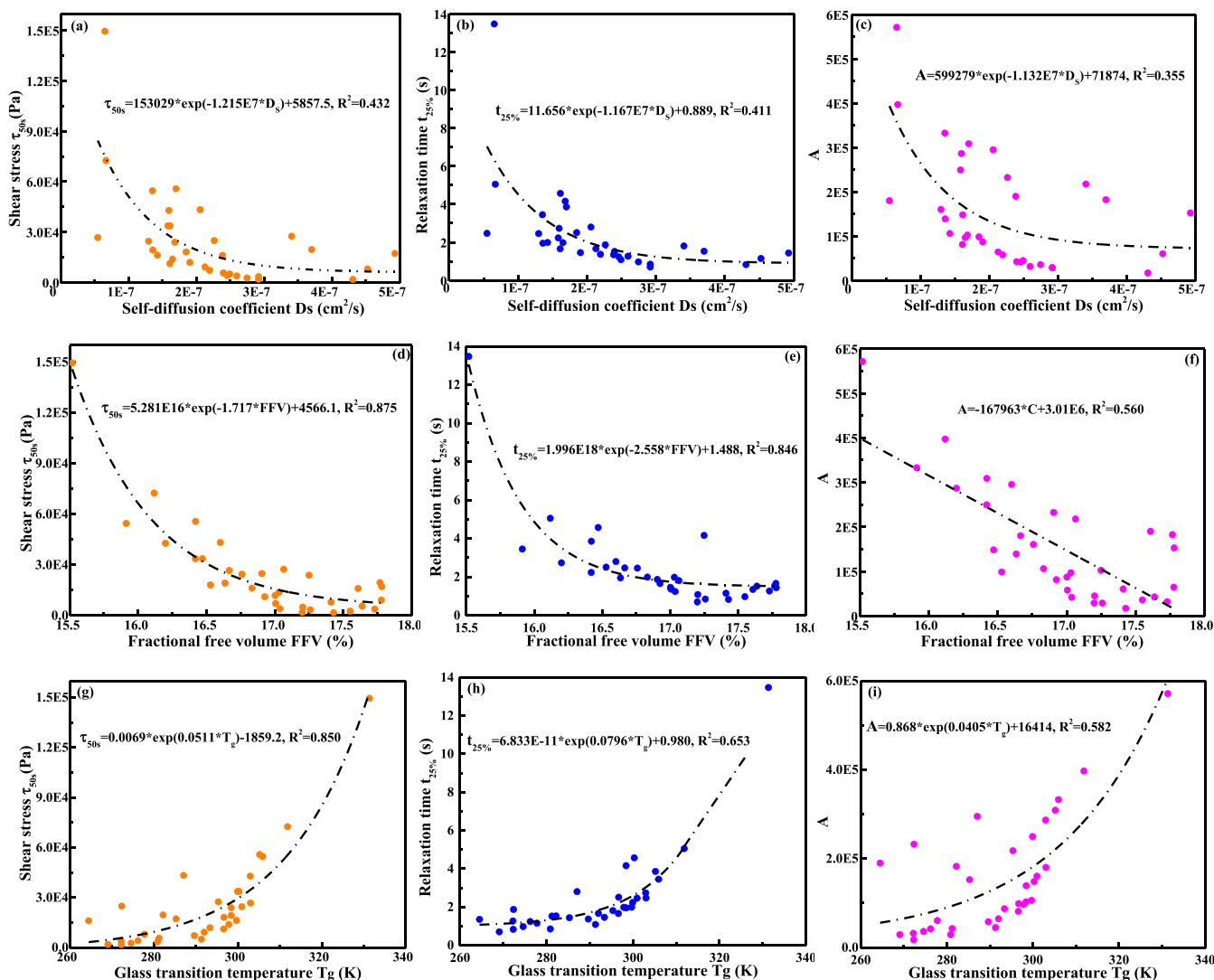


Fig. 24. Connections between low-temperature critical parameters with thermodynamic properties.

observed only in cases of virgin, aged, and aromatic-oil rejuvenated bitumen, with no evident connection noted for BORB, EORB, and NORB. This discrepancy arises from the fact that aromatic oil functions as a rejuvenator in the recovery of  $G_c$  for aged bitumen, while others such as bio-oil, engine oil, and naphthenic oil primarily act as softeners. Therefore, it becomes imperative to distinguish between rejuvenators and softeners when assessing and elucidating the efficacy of different recycling agents in the rejuvenation process.

## 7.2. Fatigue cracking performance correlation

The potential correlations between the  $\gamma$  values predicted from MD simulations and critical fatigue parameters (fatigue failure temperature FFT, fatigue life  $N_{f5}$ , elastic modulus E, peak strain  $\epsilon_{sr}$ , Glover-Rowe G-R, and crack width  $C_{500}$ ) proposed in our published paper [23] are explored to link the results from different scales. The results are illustrated in Fig. 26. It is observed that all critical fatigue parameters of rejuvenated bitumen link well to the surface free energy index. As the  $\gamma$  values increase, the FFT, E, and  $C_{500}$  indicators of rejuvenated bitumen tend to decrease exponentially, whereas the  $N_{f5}$  and  $C_{500}$  values rise gradually. It suggests that the surface free energy exhibits a positive correlation with the fatigue resistance of bitumen. Therefore, these fatigue indicators of rejuvenated bitumen can be forecasted through their correlations with predicted  $\gamma$  values.

However, it should be noticed that the correlation curves of rejuvenated bitumen extremely rely on the aging level of bitumen, and the variations of FFT- $\gamma$ ,  $N_{f5}$ - $\gamma$ , E- $\gamma$ ,  $\epsilon_{sr}$ - $\gamma$ , GR- $\gamma$ , and  $C_{500}$ - $\gamma$  curves of rejuvenated binders with a variable aging level of bitumen behave differently. In general, these correlation curves tend to move left as the aging status of bitumen changes from LAB20 to LAB40 and LAB80. It shows that when the critical fatigue indicators of rejuvenated bitumen with various aging levels are the same, their  $\gamma$  values vary significantly. This could be attributed to the fact that rejuvenation is a physical process that doesn't completely revert the aged bitumen molecules to original state [33]. From a rheological viewpoint, the introduced recycling agent (RA) can render the aged bitumen more pliable and improve its fatigue resistance. However, the RA's impact on restoring the surface free energy of aged bitumen is considerably less pronounced than its influence on macroscopic indicators. Additionally, the data points of virgin bitumen and short-term aged bitumen are out of any correlation curves, which results from the difference in bitumen aging degree. In summary, while these recycling agents (RAs) can effectively rejuvenate the macroscopic rheological properties of aged bitumen, their ability to restore the chemical characteristics, such as functional groups and surface free energy, remains constrained.

To date, it is recommended to specify the aging degree of bitumen in rejuvenated binders when these correlation laws between the surface free energy and critical fatigue indicators are used to predict the

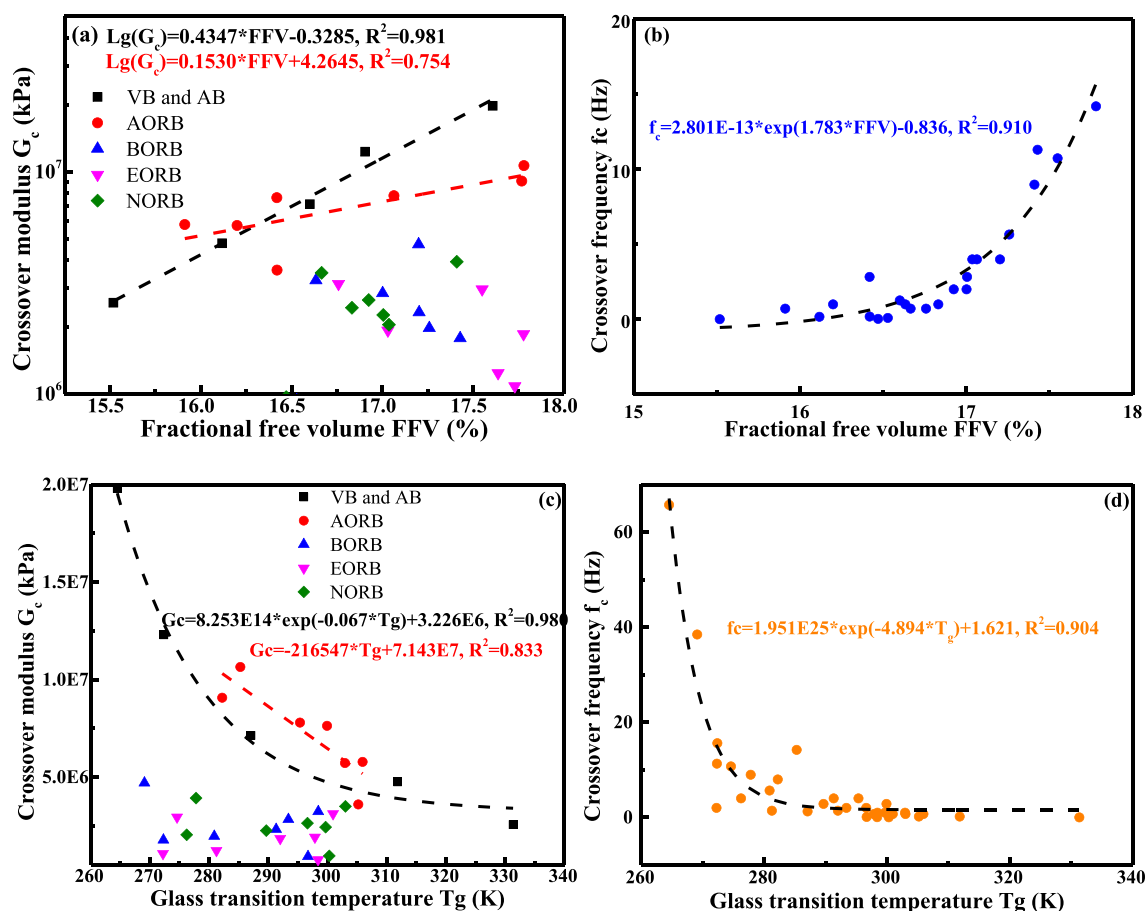


Fig. 25. Connections between crossover parameters with thermodynamic indices.

rejuvenation effectiveness of various RAs on the fatigue performance of aged bitumen. Regardless of whether it is virgin, aged, or rejuvenated bitumen, it is observed that the G-R value show an exponentially increasing trend as a function with their surface free energy value. The good connection can help predict the G-R value of rejuvenated bitumen with the  $\gamma$  result from MD simulations. Similarly, the general correlation curve between the  $C_{500}$  and  $\gamma$  parameters is created and shown in Fig. 26 (f). It is observed that the  $C_{500}$  index associates well with the  $\gamma$  values of virgin, aged, and rejuvenated bitumen with a correlation coefficient  $R^2$  value of 0.829. It means that the relationship between the  $C_{500}$  index measured from experiments and  $\gamma$  value predicted from MD simulations of bitumen is independent of the RA type/dosage and aging degree of bitumen and can be utilized in other rejuvenated bitumen cases.

## 8. Conclusions

In this study, MD simulations are implemented to assess the effects of recycling agent (RA) type/dosage and bitumen aging level on the thermodynamic properties of rejuvenated bitumen. Meanwhile, the effective thermodynamic parameters for rejuvenation efficiency evaluation are proposed. Further, the potential connections between predicted thermodynamic indices with critical low-temperature and fatigue indicators of rejuvenated bitumen are explored. The main conclusions are drawn as follows:

(1) The addition of recycling agents (RAs) significantly enlarges the free volume of aged bitumen with an efficiency order of BO > EO > NO > AO. All RAs play a positive role in improving the molecular mobility of aged bitumen, but it is necessary to mention the simulation temperature and RA dosage when ranking the rejuvenation efficiency. The BO exhibits the strongest effect on restoring the  $E_D$  value of aged bitumen,

followed by NO, AO, and EO.

(2) Adding RAs can significantly restore the  $T_g$  parameter, thus improving the low-temperature performance of aged bitumen. When the RA dosage is the same, the order of  $T_g$  values for rejuvenated bitumen is BORB < EORB < NORB < AORB. However, the addition of RAs even with the dosage of 15 % fails to completely restore the  $T_g$  value. Besides, the  $E_N$ -based  $T_g$  index is more appropriate to be an effective indicator than FV-based.

(3) High RA dosage promotes the enhancement of  $\gamma$  and cracking resistance of rejuvenated bitumen. When the RA dosage is the same, the magnitude of  $\gamma$  values for rejuvenated binders is BORB > EORB > NORB > AORB. It agrees well with the experimental fatigue conclusion. Overall, the surface free energy  $\gamma$  is an effective index to evaluate the rejuvenation efficiency of various RAs on the cohesive cracking potential of aged bitumen.

(4) The shear stress  $\tau_{50s}$  shows greater connections with thermodynamics indices than the relaxation time  $t_{25\%}$ . The FFV parameter exhibits a greater correlation with  $\tau_{50s}$  and  $t_{25\%}$  than  $T_g$ . Thus, it is recommended to predict the relaxation properties of various rejuvenated bitumen using the fractional free volume (FFV) from MD simulations. The  $T_g$  value of bitumen is affected by both FFV and molecular mobility ( $D_s$ ), while the FFV and  $D_s$  indices are interactive at the atomic level.

(5) When predicting rejuvenation efficiency for improving aged bitumen's fatigue performance, specify the aging degree in the binders. The correlation between G-R and  $C_{500}$  parameters from experiments and  $\gamma$  from MD simulations holds steady, regardless of RA type, dosage, or bitumen aging level.

(6) While these thermodynamic indicators effectively evaluate the rejuvenating efficiency of recycling agents, they fall short in

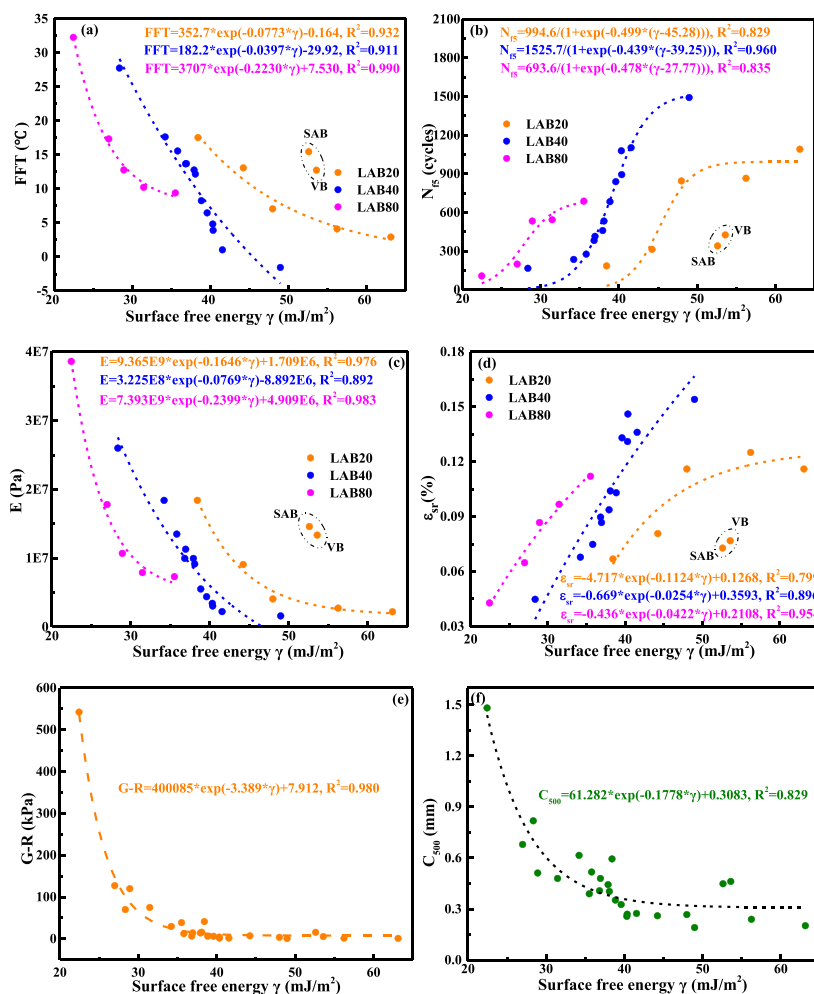


Fig. 26. Connections between fatigue critical parameters with surface free energy.

distinguishing between rejuvenators and softeners. According to the results of the crossover parameter, the majority of recycling agents examined in this study, including bio-oil, engine-oil, and naphthenic-oil, exhibit characteristics of softeners. Only aromatic-oil demonstrates the ability to revive the  $G_c$  index of aged binder. Notably, engine-oil exhibits the least rejuvenation in terms of crossover parameters for the recovery of aged bitumen. Combining bio-oil and aromatic-oil molecules proves effective in restoring molecular conformation, as it helps to deagglomerate asphaltene sheets and balance chemical components by increasing aromatic fractions in aged binder.

In future research, it's crucial to assess the applicability of these key low-temperature and fatigue indicators in various rejuvenation scenarios involving different RAs like tall-oil and polymer-modified bitumen [29,30]. In addition, the influence of various RAs on the molecular structures and moisture susceptibility of aged bitumen components should be further explored to adequately define and differentiate softening from rejuvenation [31,32]. Lastly, the proposed molecular-scale indicators for the relaxation and fatigue performance evaluation of rejuvenated bitumen need validation and optimization under various material and environmental conditions [33].

#### CRediT authorship contribution statement

**Shisong Ren:** Writing – original draft, Software, Methodology, Investigation, Formal analysis, Data curation. **Xueyan Liu:** Writing – review & editing, Supervision, Project administration. **Sandra Erkens:** Writing – review & editing, Resources, Project administration, Funding

acquisition.

#### Declaration of competing interest

The authors declare that they have no known competing financial interests or personal relationships that could have appeared to influence the work reported in this paper.

#### Data availability

Data will be made available on request.

#### Acknowledgement

The first author would thank the China Scholarship Council for the funding support (CSC, No.201906450025).

#### Appendix A. Supplementary data

Supplementary data to this article can be found online at <https://doi.org/10.1016/j.fuel.2024.131658>.

#### References

- [1] Road Pavement Transition Path. <https://www.duurzame-infra.nl/roadmaps-uitvoering/transitiepad-wegverharding>.
- [2] Towards climate-neutral and circular government infrastructure projects. Ministry of Infrastructure and Water Management. <https://www.duurzame-infra.nl>.

- [3] Rajib A, Samieadel A, Zalgout A, Kaloush K, Sharma B, Fini E. Do all rejuvenators improve asphalt performance? *Road Materials and Pavement Design* 2022;23(2): 358–76.
- [4] Yang X, Zhang H, Zheng W, Chen Z, Shi C. A novel rejuvenating method for structural and performance recovery of aged SBS-modified bitumen. *ACS Sustain Chem Eng* 2022;10(4):1565–77.
- [5] Schwettmann K, Nyttus N, Weigel S, Radenberg M, Stephan D. Effects of rejuvenators on bitumen ageing during simulated cyclic reuse: A review. *Resour Conserv Recycl* 2023;190:106776.
- [6] Moraes R, Yin F, Rodezno C. Laboratory performance and compositional evaluation of bio-based recycling agents. *Transp Res Rec* 2023;1–13.
- [7] Bocci E, Prospero E, Marsac P. Evolution of rheological parameters and apparent molecular weight distribution in the bitumen from reclaimed asphalt with rejuvenation and re-ageing. *Road Materials and Pavement Design* 2022;23(S1): S16–35.
- [8] Shariati S, Aldagari S, Fini E. Bio-modifier: a sustainable suturing technology at the bitumen-aggregate interface. *ACS Sustain Chem Eng* 2023;11(24):8908–15.
- [9] Rajib A. Structure-property relationships to understand comprehensive rejuvenation mechanisms of aged asphalt binder. Doctoral dissertation 2020.
- [10] Yu H, Ge J, Qian G, Zhang C, Dai W, Li P. Evaluation on the rejuvenation and diffusion characteristics of waste cooking oil on aged SBS asphalt based on molecular dynamics method. *J Clean Prod* 2023;406:136998.
- [11] Yan S, Dong Q, Chen X, Zhao X, Wang X. Performance evaluation of waste cooking oil at different stages and rejuvenation effect of aged asphalt through molecular dynamics simulations and density functional theory calculations. *Constr Build Mater* 2022;350:128853.
- [12] Bao C, Zheng C, Xu Y, Nie L, Wang Y. Role of rejuvenator properties in determining the activation effects on aged asphalt based on molecular simulations. *J Clean Prod* 2023;405:136970.
- [13] Cui B, Gu X, Hu D, Dong Q. A multiphysics evaluation of the rejuvenator effects on aged asphalt using molecular dynamics simulations. *Journal of Cleaner Productions* 2020;259:120629.
- [14] Zhang X, Zhou X, Chen L, Lu F, Zhang F. Effects of poly-sulfide regenerant on the rejuvenated performance of SBS modified asphalt-binder. *Mol Simul* 2021;47(17): 1423–32.
- [15] Qu X, Wang D, Hou Y, Oeser M, Wang L. Influence of paraffin on the microproperties of asphalt binder using MD simulation. *J Mater Civ Eng* 2018;30(8):04018191.
- [16] Sonibare K, Rucker G, Zhang L. Molecular dynamics simulation on vegetable oil modified model asphalt. *Constr Build Mater* 2021;270:121687.
- [17] Ding H, Wang H, Qu X, Varveri A, Gao J, You Z. Towards an understanding of diffusion mechanism of bio-rejuvenators in aged asphalt binder through molecular dynamics simulation. *J Clean Prod* 2021;299:126927.
- [18] Zadshir M, Oldham D, Hosseinezhad S, Fini E. Investigating bio-rejuvenation mechanisms in asphalt binder via laboratory experiments and molecular dynamics simulation. *Constr Build Mater* 2018;190:392–402.
- [19] Zhang X, Ning Y, Zhou X, Xu X, Chen X. Quantifying the rejuvenation effects of soybean-oil on aged asphalt-binder using molecular dynamics simulations. *J Clean Prod* 2021;317:128375.
- [20] Gong M, Jiao B. Thermodynamic properties analysis of warm-mix recycled asphalt binders using molecular dynamics simulation. *Road Materials and Pavement Design* 2023;2199883.
- [21] Li D, Ding Y, Wang J, Shi Y, Cao Z, Sun G, et al. Multiscale molecular simulations on the rejuvenation of recycled asphalt mixture: an insight into molecular impact of rejuvenators in aged binders. *J Clean Prod* 2023;414:137621.
- [22] Ren S, Liu X, Aggelen M, Lin P, Erkens S. Do different chemical and critical indicators for efficiency evaluation of rejuvenated bitumen. *Constr Build Mater* 2024;411:134774.
- [23] Ren S, Liu X, Erkens S. Insight into the critical evaluation indicators for fatigue performance recovery of rejuvenated bitumen under different rejuvenation conditions. *Int J Fatigue* 2023;175:107753.
- [24] Ren S, Liu X, Erkens S. Towards critical low-temperature relaxation indicators for effective rejuvenation efficiency evaluation of rejuvenator-aged blends. *J Clean Prod* 2023;426:139092.
- [25] Ren S, Liu X, Lin P, Erkens S, Xiao Y. Chemo-physical characterization and molecular dynamics simulation of long-term aging behaviors of bitumen. *Constr Build Mater* 2021;302:124437.
- [26] Ren S, Liu X, Lin P, Jing R, Erkens S. Toward the long-term aging influence and novel reaction kinetics models of bitumen. *Int J Pavement Eng* 2022.
- [27] S. Ren, X. Liu, P. Lin, S. Erkens, Y. Gao. Chemical characterizations and molecular dynamics simulations on different rejuvenators for aged bitumen recycling. 2022, *Fuel*. 324, Part A, 124550.
- [28] Apostolidis P, Elwardany M, Porot L, Vansteenkiste S, Chailleux E. Glass transitions in bituminous binders. *Mater Struct* 2021;54:132.
- [29] Han X, Mao S, Xu S, Cao Z, Zeng S, Yu J. Development of novel composite rejuvenators for efficient recycling of aged SBS modified bitumen. *Fuel* 2022;318: 123715.
- [30] Cong P, Guo X, Mei L. Investigation on rejuvenation methods of aged SBS modified asphalt binder. *Fuel* 2020;279:118556.
- [31] Pahlavan F, Hosseinezhad S, Samieadel A, Hung A, Fini E. Fused aromatics to restore molecular packing of aged bituminous materials. *Ind Eng Chem Res* 2019; 58:11939–53.
- [32] Rajib A, Pahlavan F, Fini E. Investigating molecular-level factors that affect the durability of restored aged asphalt binder. *J Clean Prod* 2020;270:122501.
- [33] Hung A, Goodwin A, Fini E. Effects of water exposure on bitumen surface microstructure. *Constr Build Mater* 2017;135:682–8.
- [34] Oldham D, Obando C, Mousavi M, Kaloush K, Fini E. Introducing the critical aging point (CAP) of asphalt based on its restoration capacity. *Constr Build Mater* 2021; 278:122379.
- [35] Oldham D, Rajib A, Dandamudi K, Liu Y, Deng S, Fini E. Transesterification of waste cooking oil to produce a sustainable rejuvenator for aged asphalt. *Resour Conserv Recycl* 2021;168:105297.
- [36] Pahlavan F, Rajib A, Deng S, Lammers P, Fini E. Investigation of balanced feedstocks of lipids and proteins to synthesize highly effective rejuvenators for oxidized asphalt. *ACS Sustain Chem Eng* 2020;8:7656–67.